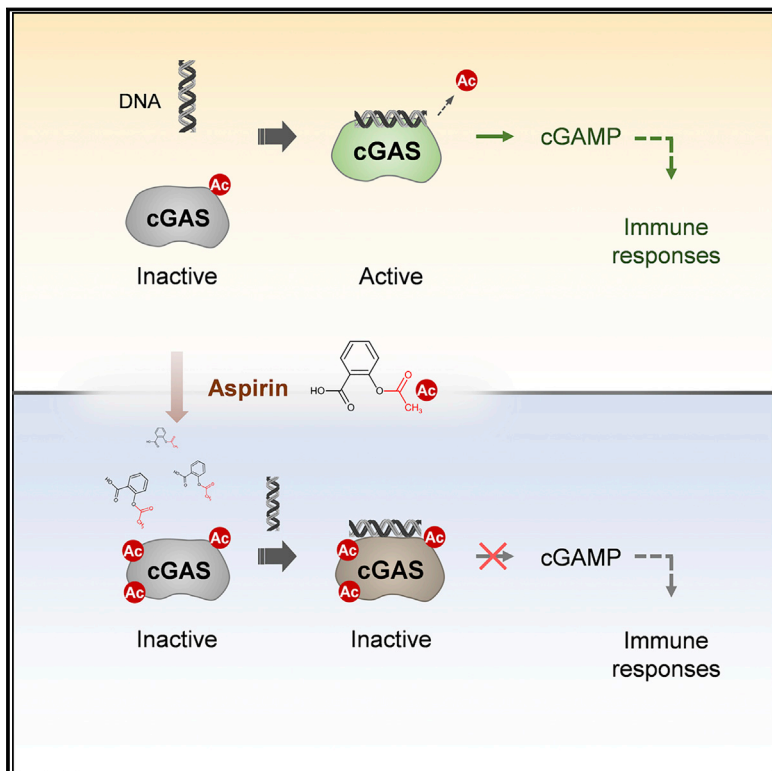# Cell

Acetylation Blocks cGAS Activity and Inhibits Self-DNA-Induced Autoimmunity

Graphical Abstract

Authors

Jiang Dai, Yi-Jiao Huang, Xinhua He, ..., Zheng-Gang Liu, Xue-Min Zhang, Tao Li

Correspondence

zhangxuemin@cashq.ac.cn (X.-M.Z.),
tli@ncba.ac.cn (T.L.)

In Brief

Activation of the DNA sensor cGAS requires a deacetylation step, and its aspirin-induced acetylation can limit innate immune responses.

Highlights

- Acetylation suppresses cGAS activity

- Aspirin directly acetylates cGAS

- Aspirin inhibits cGAS-mediated interferon production

- Aspirin alleviates DNA-induced autoimmunity in AGS mouse models and patient cells

CellPress

Article

Acetylation Blocks cGAS Activity and Inhibits Self-DNA-Induced Autoimmunity

Jiang Dai,[1,2,6] Yi-Jiao Huang,[2,6] Xinhua He,[1,6] Ming Zhao,[2] Xinzheng Wang,[2] Zhao-Shan Liu,[2] Wen Xue,[2] Hong Cai,[2] Xiao-Yan Zhan,[2] Shao-Yi Huang,[1,2] Kun He,[2] Hongxia Wang,[2] Na Wang,[2] Zhihong Sang,[2] Tingting Li,[2] Qiu-Ying Han,[2] Jie Mao,[2] Xinwei Diao,[2,3] Nan Song,[2] Yuan Chen,[2] Wei-Hua Li,[2] Jiang-Hong Man,[2] Ai-Ling Li,[2] Tao Zhou,[2] Zheng-Gang Liu,[4] Xue-Min Zhang,[1,2,5,*] and Tao Li[1,2,7,*]

[1]State Key Laboratory of Toxicology and Medical Countermeasures, Institute of Pharmacology and Toxicology, National Center of Biomedical Analysis, 27 Tai-Ping Road, Beijing 100850, China
[2]State Key Laboratory of Proteomics, Institute of Basic Medical Sciences, National Center of Biomedical Analysis, 27 Tai-Ping Road, Beijing 100850, China
[3]Department of Pathology, Xinqiao Hospital, 3rd Military Medical University, Chongqing 400037, China
[4]Center for Cancer Research, National Cancer Institute, NIH, Bethesda, MD 20892, USA
[5]Cancer Research Institute of Jilin University, the First Hospital of Jilin University, Changchun, Jilin Province 130021, China
[6]These authors contributed equally
[7]Lead Contact
*Correspondence: zhangxuemin@cashq.ac.cn (X.-M.Z.), tli@ncba.ac.cn (T.L.)
https://doi.org/10.1016/j.cell.2019.01.016

SUMMARY

The presence of DNA in the cytoplasm is normally a sign of microbial infections and is quickly detected by cyclic GMP-AMP synthase (cGAS) to elicit anti-infection immune responses. However, chronic activation of cGAS by self-DNA leads to severe autoimmune diseases for which no effective treatment is available yet. Here we report that acetylation inhibits cGAS activation and that the enforced acetylation of cGAS by aspirin robustly suppresses self-DNA-induced autoimmunity. We find that cGAS acetylation on either Lys384, Lys394, or Lys414 contributes to keeping cGAS inactive. cGAS is deacetylated in response to DNA challenges. Importantly, we show that aspirin can directly acetylate cGAS and efficiently inhibit cGAS-mediated immune responses. Finally, we demonstrate that aspirin can effectively suppress self-DNA-induced autoimmunity in Aicardi-Goutières syndrome (AGS) patient cells and in an AGS mouse model. Thus, our study reveals that acetylation contributes to cGAS activity regulation and provides a potential therapy for treating DNA-mediated autoimmune diseases.

INTRODUCTION

Cytosolic DNA is a potent danger signal that triggers robust innate immune responses because the presence of DNA in the cytoplasm is normally a sign of microbial infection or tissue damage (Barbalat et al., 2011). Recognition of cytosolic DNA is an important mechanism for host defense. Cyclic guanosine monophosphate (GMP)-AMP synthase (cGAS) has been identified as a key sensor that mediates immune responses upon cytoplasmic DNA challenge. Upon DNA binding, the activated cGAS cata-

lyzes the synthesis of cyclic GMP-AMP (cGAMP) from ATP and guanosine triphosphate (GTP) (Gao et al., 2013; Sun et al., 2013; Wu et al., 2013b). cGAMP then acts as a second messenger to bind and activate the endoplasmic reticulum protein STING (also known as MITA, MPYS, and ERIS) (Ishikawa and Barber, 2008; Jin et al., 2008; Sun et al., 2009; Zhong et al., 2008), which, in turn, mediates the activation of the downstream effectors TANK-binding kinase 1 (TBK1) and interferon regulatory factor 3 (IRF3) to produce type I interferon (IFN) (Bowie, 2012). Type I IFN plays critical roles in antiviral responses by inducing the expression of a number of interferon-stimulated genes (ISGs) (Gao et al., 2015).

In addition to microbial infection, cellular damage or reverse transcription of endogenous retroviruses can also generate self-DNA in the cytoplasm (Ahn and Barber, 2014; Kassiotis and Stoye, 2016; O'Neill, 2013). Metazoans have evolved DNases that clear self-DNA to prevent inappropriate activation of cGAS-mediated immune responses. For example, DNA 3′ repair exonuclease 1 (TREX1) degrades cytosolic DNA, and loss-of-function mutations of *TREX1* have been identified in human patients with autoimmune disorders such as Aicardi-Goutières syndrome (AGS) and lupus (Ahn and Barber, 2014; Aicardi and Goutières, 1984; Crow and Manel, 2015; Lisnevskaia et al., 2014). AGS patients harboring *TREX1* mutations are known to accumulate cytoplasmic self-DNAs that chronically stimulate cGAS-mediated type I IFN production (Crow et al., 2006; Gao et al., 2015; Gray et al., 2015; Stetson et al., 2008). The excessively produced IFN drives systemic inflammation and other autoimmune responses (Elkon and Wiedeman, 2012). Deletion of *Trex1* in mice results in severe cGAS-dependent autoimmunity because deletion of *Cgas* rescues the lethality and autoimmune conditions in *Trex1*^{−/−} mice (Gao et al., 2015; Gray et al., 2015). These studies suggest that cGAS inhibition could be used for treating self-DNA-mediated autoimmune diseases. A limited understanding of how cGAS activation is regulated, however, has prevented the development of effective treatments.

Cell

Post-translational modifications (PTMs) such as acetylation and phosphorylation are known to be critical for regulation of protein functions (Cohen, 2000; Verdin and Ott, 2015). Protein acetylation plays important roles in various biological processes, including immune responses (Shakespear et al., 2011). In the current study, we found that acetylation at one of three lysine residues, Lys384, Lys394, or Lys414, contributes to keeping cGAS inactive. cGAS is deacetylated in response to DNA challenge. Importantly, we show that aspirin, a drug that is well-tolerated in humans, can robustly enforce the acetylation of cGAS and led to cGAS inhibition. Furthermore, we demonstrate that aspirin ameliorates DNA-mediated autoimmune responses in mice and in AGS patient cells.

RESULTS

Acetylation-Mimicking Mutation of cGAS Blocks cGAS Activation

Because acetylation is a key PTM that plays important roles in many biological processes (Verdin and Ott, 2015), and acetylation of cGAS in quiescent cells has been implied in proteomic studies (Choudhary et al., 2009; Zhao et al., 2010), we investigated whether acetylation is involved in the regulation of cGAS activity. To do so, we first created a FLAG-cGAS stable THP-1 (human monocytic cells) cell line and examined cGAS acetylation in quiescent cells by performing liquid chromatography-mass spectrometry (LC-MS) with the immunoprecipitated FLAG-cGAS. We identified six lysine (K) acetylation sites of cGAS: K7, K50, K384, K392, K394, and K414 (Figure S1A). Interestingly, three of these six sites are conserved across species (Figure S1B). To study the function of acetylation of these sites, we mutated each site by replacing a lysine with a glutamine (Q), which mimics the acetylation state on lysine (Zhao et al., 2010), and tested the effect of these mutations on cGAS activity in HEK293T cells that stably express STING (Sun et al., 2013). cGAS-STING pathway activation can be reflected by phosphorylation of the downstream transcription factor IRF3 (Sun et al., 2013). We found that K-to-Q mutation of each of the three conserved sites K384, K394 or K414 (cGAS^{K384Q}, cGAS^{K394Q}, or cGAS^{K414Q})—led to a dramatic reduction in cGAS activity, whereas the mutations of the non-conserved sites—cGAS^{K7Q}, cGAS^{K50Q}, or cGAS^{K392Q}—had no effect (Figure 1A). By replacing a lysine with an arginine (R), we further found that K-to-R mutation of K384 or K394 did not affect cGAS activation, whereas substitution of K414 with R also inhibited cGAS activity (Figure 1B). These data suggest that, although K414 appeared to be a critical residue of cGAS, acetylation on these conserved lysine sites could possibly inhibit cGAS activation. Next we used CRISPR/Cas9 to delete endogenous cGAS in THP-1 cells. As expected, these cells failed to induce IRF3 phosphorylation and IFN production upon stimulation by introducing herring testis DNA (HT-DNA) into the cells. This deficiency could be rescued by wild-type cGAS but not acetylation-mimicking cGAS (Figures 1C and 1D). Using simultaneous K-to-Q mutation of cGAS on K384, K394, and K414 (cGAS^{3KQ}), we obtained similar results (Figures 1E and 1F). These data further suggest that acetylation may inhibit cGAS activation.

To study the activity of cGAS in the above cells, we used LC-MS/multiple reaction monitoring (LC-MS/MRM) to measure the production of cGAMP (Figure S1C). In contrast to wild-type cGAS, the acetylation-mimicking cGAS mutants cGAS^{K384Q}, cGAS^{K394Q}, cGAS^{K414Q}, and cGAS^{3KQ} failed to synthesize cGAMP upon stimulation by the introduced HT-DNA (Figures 1G and 1H).

Acetylation Suppresses cGAS Activity

To unambiguously determine the effect of acetylation on cGAS at these residues, we utilized a system to genetically incorporate acetyl-lysine into a recombinant cGAS protein (Neumann et al., 2008) at each of the conserved sites to create cGAS^{Lys384Ac}, cGAS^{Lys394Ac}, and cGAS^{Lys414Ac} (Figure 2A). We also created cGAS^{Lys392Ac} as a control because the K392Q mutation did not inhibit cGAS activation (Figure 1A). Additionally, we generated site-specific anti-acetylation antibodies using the peptides FSHIEK(384)^{Ac}EILNNHGKSK(394)^{Ac}T and RKDCLKLMK(414)^{Ac}YLLEQ to detect the K384 and/or K394 and K414 acetylated human cGAS, respectively (Figure 2B). We performed an *in vitro* cGAMP synthesis assay by incubating the acetylated cGAS proteins cGAS^{Lys384Ac}, cGAS^{Lys394Ac}, or cGAS^{Lys414Ac} with the substrates ATP and GTP in the presence of HT-DNA. Consistent with the K-to-Q mutation results, cGAS^{Lys384Ac}, cGAS^{Lys394Ac}, or cGAS^{Lys414Ac} failed to synthesize cGAMP, whereas the unmodified cGAS (cGAS^{Non-Ac}) and cGAS^{Lys392Ac} effectively produced cGAMP (Figures 2C, S2A, and S2B). Thus, these data suggest that acetylation may inhibit cGAS activity.

Previous structural studies suggested that these sites (K384, K394, and K414) are involved in the DNA binding of cGAS (Gao et al., 2013; Kranzusch et al., 2013; Li et al., 2013; Figure S2C). We then tested the above acetylated cGAS proteins for their DNA-binding ability using biolayer interferometry and found that single-site acetylation of cGAS slightly reduced cGAS-DNA binding affinity (Figures 2D and S2D). These data are consistent with a previous report showing that the mutations on some of these sites had only a limited effect on DNA binding of cGAS (Li et al., 2013). Next we detected whether cGAS mutations affect the dimerization of cGAS because cGAS is known to bind to DNA as a dimer (Zhang et al., 2014). To do so, FLAG-tagged wild-type cGAS was expressed in HEK293T cells. The cell lysates were then incubated with recombinant His-tagged cGAS proteins: cGAS^{Non-Ac}, cGAS^{Lys384Ac}, cGAS^{Lys394Ac}, or cGAS^{Lys414Ac}. The cGAS-cGAS interaction were examined by pulling down His-tagged cGAS protein and immunoblotting with anti-FLAG antibody. Our data showed that cGAS dimerization was not likely to be affected by cGAS acetylation (Figure 2E). Using the cGAS K-to-Q mutant-rescued cell lines, we found that these acetylation-mimicking mutants had similar protein stability and localization compared with that of wild-type cGAS (Figures 2F and 2G). It is possible that acetylation interferes with cGAS enzymatic activity.

Deacetylation of cGAS upon DNA Treatment Is Involved in cGAS Activation

To explore how cGAS acetylation is regulated in response to DNA challenge, we treated FLAG-cGAS stable THP-1 cells with HT-DNA and checked the acetylation of cGAS with site-specific antibodies. We found that acetylation of cGAS on K384 and/or
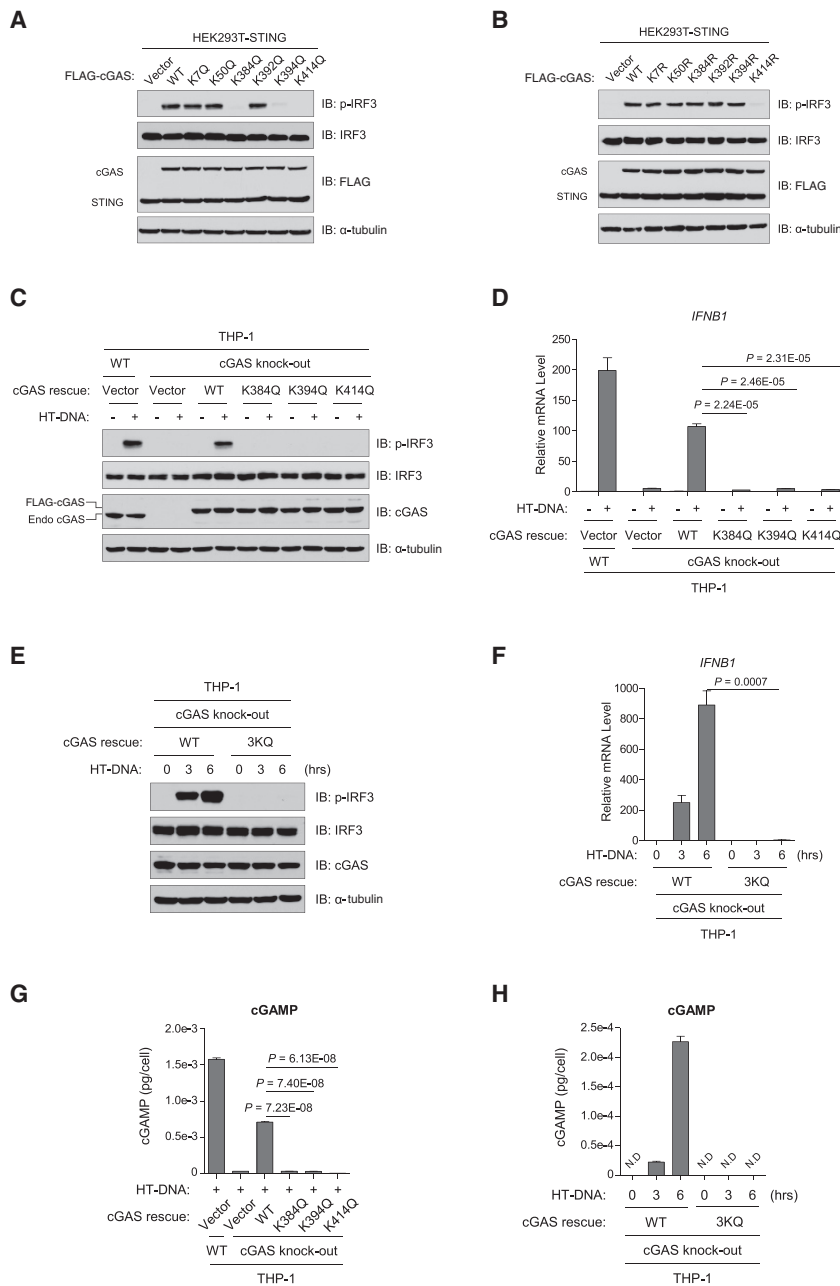
Cell

Figure 1. Acetylation Inhibits cGAS-Mediated Type I IFN Production

(A and B) Plasmids encoding FLAG-tagged wild-type (WT) human cGAS and its acetylation-mimetic (K-to-Q) mutants (A) or K-to-R mutants (B) were transfected into HEK293T cells that stably expressed STING (HEK293T-STING). Shown is immunoblot analysis of phosphorylation of IRF3 in the cells.

(C–H) cGAS knockout THP-1 cells were infected with a lentivirus carrying WT or acetylation-mimetic cGAS to make cell lines expressing different cGAS mutants. The cells were differentiated with phorbol-12-myristate-13-acetate (PMA) for 72 h, followed by transfection of HT-DNA (2 μg/mL) for 6 h (C and D) or 3 h (G) or for the indicated time (E, F, and H). IRF3 phosphorylation was detected by immunoblotting (C and E). Total RNAs were extracted, and the *IFNB1* mRNA levels were analyzed by qPCR (D and F). The production of cGAMP was detected by LC-MS/MRM. Data are mean ± SEM from triplicates (technical replicates); unpaired t test (D and F–H).

Anti-α-tubulin (A–C and E) blots indicate loading of lanes. Data represent at least three independent experiments.

See also Figure S1.

noprecipitated complex by LC-MS analysis, we found that HDAC3 protein was co-precipitated with cGAS (Table S1). This interaction of cGAS and HDAC3 was confirmed by western blotting (Figure S3D). As reported previously, the nuclear deacetylase HDAC3 can also localize in the cytoplasm (Yuan et al., 2005), and we found that the interaction of HDAC3 and cGAS is stabilized by DNA treatment (Figures 3C and 3D). Importantly, knockdown of HDAC3 prevented deacetylation of cGAS in response to HT-DNA stimuli and attenuated DNA-induced IRF3 phosphorylation (Figure 3E). Consistently, knockdown of HDAC3 also reduced HT-DNA-induced cGAMP production in cells (Figure S3E). These data suggest that acetylation contributes to cGAS activity inhibition and

K394 and K414 was reduced after HT-DNA treatment (Figure 3A), suggesting that DNA treatment leads to deacetylation of cGAS. This was confirmed by examining the acetylation of the endogenous cGAS protein in response to HT-DNA treatment and infection with herpes simplex virus (HSV)-1, a DNA virus (Figures 3B and S3A). Using MS to analyze cGAS acetylation before and after DNA virus or HT-DNA treatment, our data further supported the above observations (Figures S3B and S3C; Table S2).

It is known that deacetylation is mediated by deacetylases, sirtuins (SIRTs), and histone deacetylases (HDACs) (Shakespear et al., 2011). Interestingly, when we examined the cGAS-immu-

that deacetylation of cGAS upon DNA treatment is involved in cGAS activation.

Enforced Acetylation of cGAS by Aspirin

We next investigated whether enforced acetylation of cGAS could inhibit its activity. Aspirin, a non-steroidal anti-inflammatory drug (NSAID), is known to be able to acetylate proteins such as cyclooxygenase (COX, also known as prostaglandin-endoperoxide synthase) (Roth and Majerus, 1975; Vane and Botting, 2003). For COX acetylation, aspirin acetylates the hydroxyl group of serine and forms an ester bond (O-link). It is known that
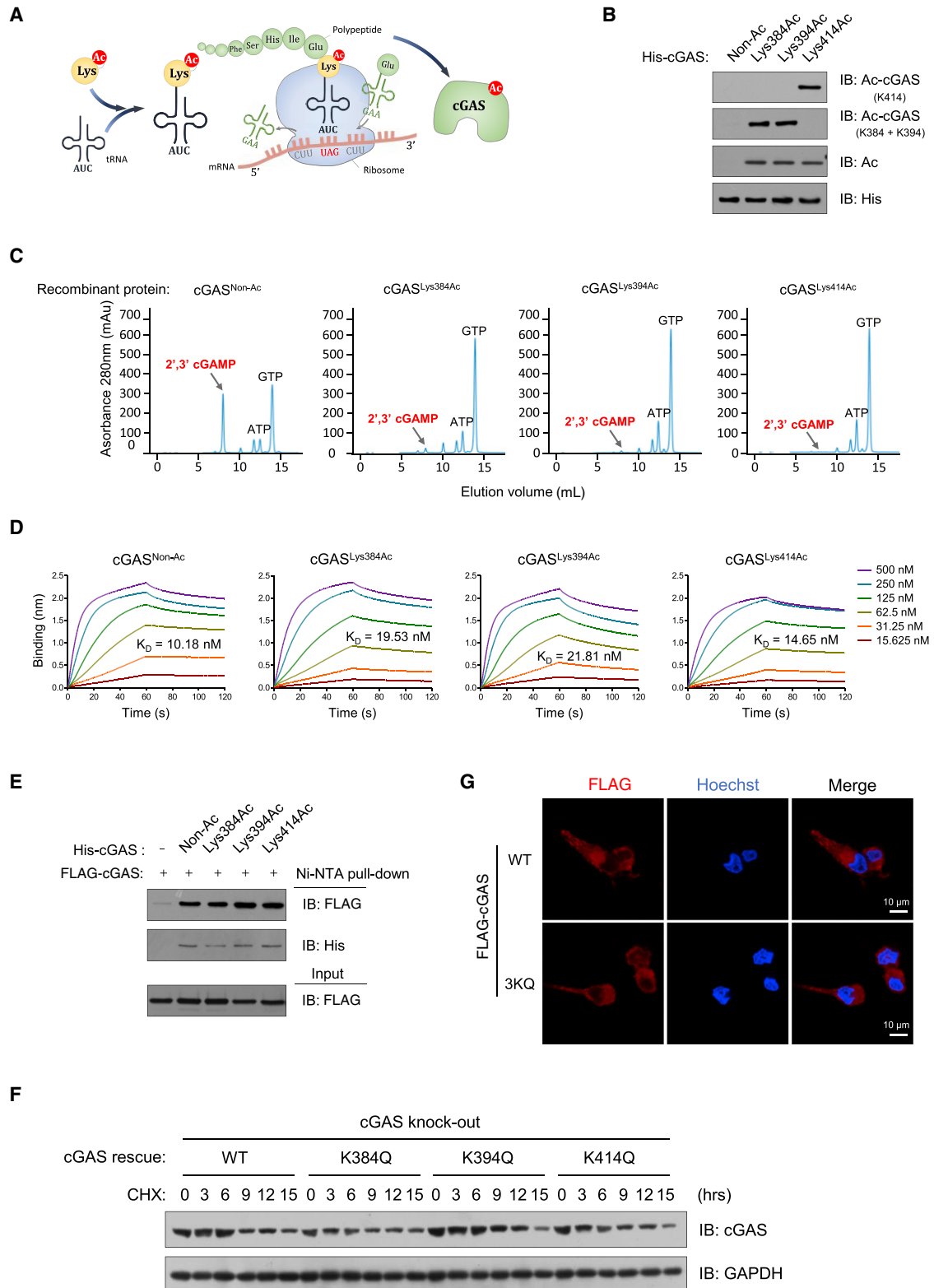
Cell

Figure 2. Acetylation Suppresses cGAS Activity

(A) A schematic describing the generation of site-specific acetylated recombinant cGAS protein with an acetyl-lysine tRNA, which incorporates the acetyl-lysine on the amber codon (uracil, adenine, guanine [UAG]).

(legend continued on next page)

amido bonds are more stable than ester bonds; we therefore hypothesized that aspirin may acetylate the amino group of lysine to form an amido bond (N-link). We then tested whether aspirin could acetylate cGAS at the above lysine sites and inhibit its activation. Apparently, aspirin is indeed able to acetylate cGAS because incubation of aspirin with the recombinant cGAS protein led to a remarkable modification of cGAS (Figure 4A). Using our site-specific cGAS acetylation antibodies, we confirmed that aspirin can acetylate cGAS recombinant protein at K384 and/or K394 and K414 (Figure 4B). By testing the cytotoxicity of aspirin, we treated THP-1, human peripheral blood mononuclear cells (PBMCs), and mouse bone marrow cells with aspirin and found that the concentration of 4 mM aspirin did not significantly affect cell viability (Figures S4A–S4C). We thus used aspirin at 4 mM to treat cells. Importantly, treating THP-1 cells with aspirin enforced acetylation of the endogenous cGAS (Figures 4C and 4D). We further found that aspirin treatment enforced and maintained the high level of cGAS acetylation, even in the presence of DNA treatment (Figure S4D). Moreover, aspirin treatment also acetylated mouse cGAS (m-cGAS) at the corresponding sites (Figure S4E; Table S2). Thus, aspirin can be used to induce inhibitory acetylation on cGAS.

To further demonstrate that aspirin can directly acetylate cGAS, we used an isotopically labeled aspirin (aspirin-d3) according to a previous report (Tatham et al., 2017). By incubating recombinant cGAS protein with aspirin-d3, we found that, similar to the regular aspirin, this isotopically labeled aspirin can directly acetylate cGAS protein (Figure 4E). We next confirmed that aspirin-d3 treatment led to a high level of cGAS acetylation with an acetyl-d3 group in cells by MS (Figures 4F–4H; Table S2). These data collectively suggest that aspirin treatment can directly induce cGAS acetylation and that aspirin could be used to inhibit cGAS activity.

Aspirin Inhibits cGAS-Mediated IFN Production

We then tested the effect of aspirin on DNA-induced activation of cGAS and found that aspirin had a significant inhibitory effect on IRF3 phosphorylation induced by the DNA virus HSV-1 but not the RNA virus vesicular stomatitis virus (VSV) (Figures 5A and 5B). We obtained a similar result using aspirin-d3 (Figure 5C). Thus, aspirin inhibits DNA-mediated activation of the cGAS-STING pathway.

To confirm that the inhibitory effect of aspirin on the cGAS-STING pathway is through inhibiting cGAS, we first tested

whether aspirin has any effect on cGAMP-mediated activation of the pathway. We found that aspirin did not inhibit cGAMP-activated phosphorylation of IRF3 and TBK1 (Figure 5D) or cGAMP-induced IFN production (Figure S5A). We then used another STING activator, cyclic diguanylate (c-di-GMP) (Burdette et al., 2011), to challenge the aspirin-treated cells and found that aspirin did not inhibit IFN production activated by c-di-GMP (Figure S5B). These data demonstrate that the inhibitory effect of aspirin is most likely through blocking cGAS activity. Consistently, aspirin suppressed cGAMP synthesis in HT-DNA-stimulated cells without significantly affecting the protein level of cGAS (Figures 5E and S5C). By incubating aspirin with recombinant cGAS protein, we found that aspirin acetylated the protein (Figure 5F) and blocked the production of cGAMP (Figure 5G). Taken together, these results suggest that aspirin acetylates cGAS and inhibits its activity.

Next, we studied whether aspirin can specifically inhibit cGAS-mediated IFN production in vivo by injecting mice with aspirin prior to HSV-1 or VSV infection. We measured the serum levels of IFN-β and found that aspirin significantly inhibited HSV-1- but not VSV-induced IFN-β production in mice (Figures 5H and 5I). Thus, aspirin blocks cGAS-mediated type I IFN production both in vitro and in vivo.

Aspirin Suppresses DNA-Mediated Autoimmunity in Mice

To determine whether aspirin could be used to treat self-DNA-induced autoimmunity, we used $Trex1^{-/-}$ mice, which exhibit similar autoimmune disorders as human patients (Morita et al., 2004). We first isolated bone marrow cells from both wild-type and $Trex1^{-/-}$ mice. As expected, $Trex1^{-/-}$ bone marrow cells showed highly elevated levels of ISGs compared with wild-type cells. Treating $Trex1^{-/-}$ bone marrow cells with aspirin strongly inhibited the expression of ISGs (Figure S6A). We further calculated the half-maximal inhibitory concentration (IC_{50}) of aspirin for suppressing ISG expression by performing a dose-response curve experiment (Figure 6A). According to a previous study (di Palma et al., 2006), we gave mice a daily aspirin injection (50 mg/kg) for 10 days and monitored the body weight of mice during the process. We observed barely any weight loss in the treated mice (Figure S6B). We then injected $Trex1^{-/-}$ mice intraperitoneally (i.p.) with aspirin to test whether aspirin has a therapeutic effect to alleviate the disease phenotype in these mice. Because it has been reported that aspirin also

(B) Immunoblot analysis of the acetylated recombinant cGAS proteins with site-specific cGAS acetylation antibodies and the pan-acetyl-lysine antibody. The anti-His blot indicates loading of lanes.

(C) Ion exchange chromatography analysis of cGAMP production from an in vitro cGAMP synthesis assay.

(D) Real-time association and dissociation of non-acetylated or acetylated recombinant cGAS proteins with biotin-EGFP (EGFP-coding DNA sequence) were recorded by ForteBio Octet red 96. Processed kinetics data show binding affinity constants (equilibrium dissociation constant, K_D).

(E) FLAG-tagged WT cGAS was expressed in HEK293T cells. The cell lysates were then incubated with recombinant His-tagged cGAS proteins, cGAS^{Non-Ac}, cGAS^{Lys384Ac}, cGAS^{Lys394Ac}, or cGAS^{Lys414Ac}. The cGAS-cGAS interaction was examined by pulling down His-tagged cGAS protein and immunoblotting with anti-FLAG antibody.

(F) cGAS knockout THP-1 cells were infected with a lentivirus carrying WT or acetylation-mimetic cGAS to make cell lines expressing different cGAS mutants. Cells were differentiated with PMA for 72 h, followed by cycloheximide (CHX) (100 μg/mL) treatment for the indicated time. cGAS was immunoblotted. The anti-GAPDH blot indicates loading of lanes.

(G) Immunofluorescence analysis of cGAS (red) in PMA-differentiated FLAG-cGAS or FLAG-cGAS^{3KQ} expressing THP-1 cells. Hoechst (blue) stained the nuclei. Data represent at least three independent experiments.
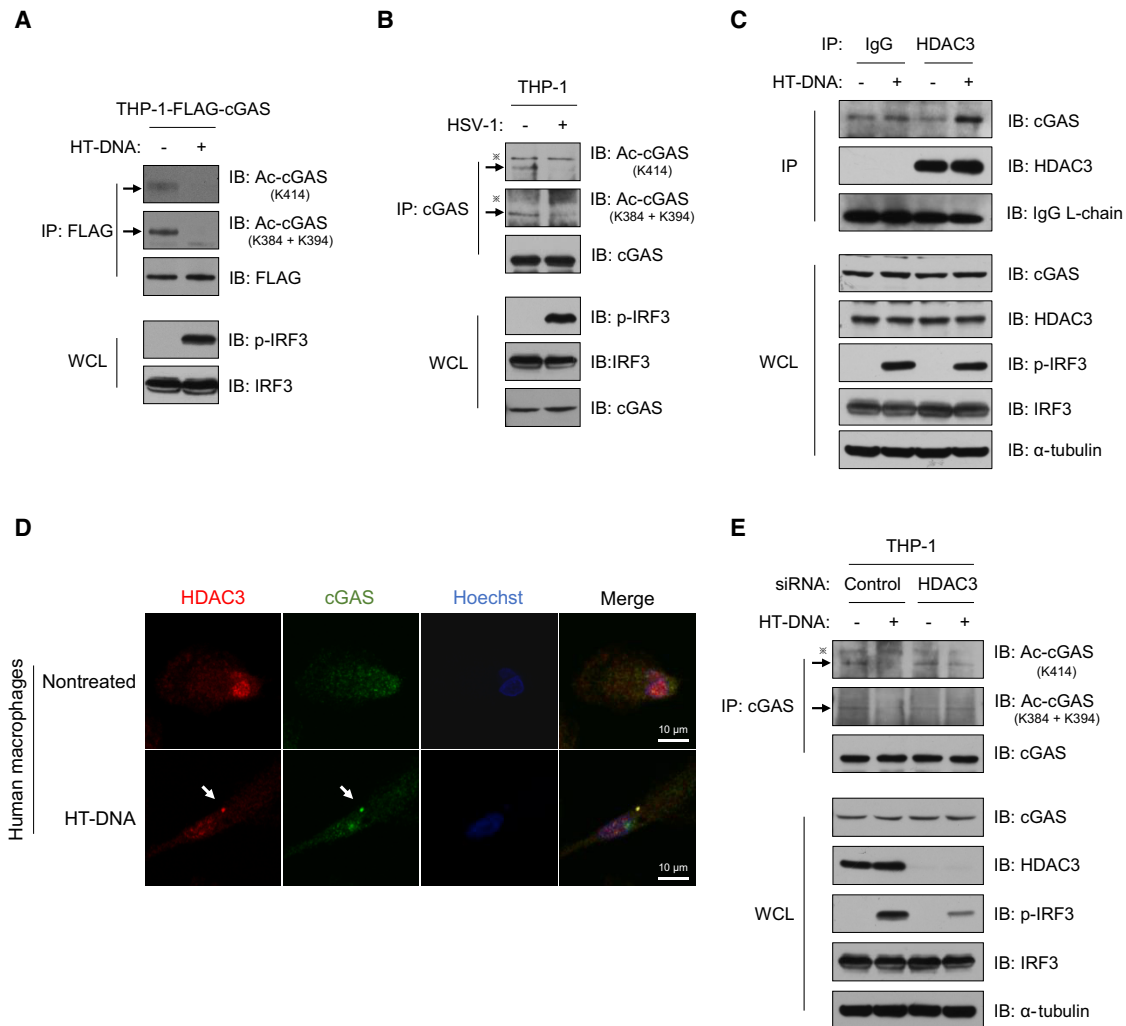
See also Figure S2.

Cell

Figure 3. Deacetylation of cGAS upon DNA Treatment Is Involved in cGAS Activation

(A) PMA-differentiated THP-1 cells that stably express FLAG-cGAS were left untreated or treated with HT-DNA (2 μg/mL) for 3 h. FLAG-cGAS was immuno-precipitated, and the acetylation of cGAS was analyzed with site-specific cGAS acetylation antibodies as indicated.

(B) PMA-differentiated THP-1 cells were infected with HSV-1 (MOI = 10:1) for 6 h. cGAS was immunoprecipitated, and the acetylation of cGAS was analyzed with site-specific cGAS acetylation antibodies as indicated.

(C) PMA-differentiated THP-1 cells were treated with HT-DNA (2 μg/mL) for 3 h. The interaction between HDAC3 and cGAS was examined by immunoprecip-itation (IP) and immunoblotting.

(D) Immunofluorescence analysis of cGAS (green) and HDAC3 (red) in human primary macrophages that were left untreated or stimulated with HT-DNA (1 μg/mL) for 2 h. Hoechst (blue) stained the nuclei.

(E) THP-1 cells were transfected with control siRNAs or HDAC3 siRNAs for 24 h, followed by PMA treatment for another 48 h. Cells were then treated with HT-DNA (2 μg/mL) for 3 h. cGAS was immunoprecipitated, and acetylation of cGAS was analyzed with site-specific cGAS acetylation antibodies.

※ indicates non-specific bands (B and E). WCL, whole cell lysate (A–C and E). Anti-α-tubulin blots indicate loading of lanes (C and E). Data represent three independent experiments.

See also Figure S3 and Table S1.

targets other inflammation-related pathways, such as COX-1 and COX-2 (Vane and Botting, 2003) and nuclear factor κB (NF-κB) (Kopp and Ghosh, 1994; Yin et al., 1998), we also used diclofenac sodium, a potent inhibitor of COX-1 and COX-2 (Grabocka and Bar-Sagi, 2016), and salicylic acid, a metabolite of aspirin (acetylsalicylic acid) (Hutt et al., 1986) known to inhibit the NF-κB pathway (Kopp and Ghosh, 1994; Yin et al., 1998), as control compounds (Figures S6C and S6D).

Because salicylic acid does not have an acetyl group, it cannot acetylate cGAS protein (Figure S6E). Consistently, salicylic acid did not obviously inhibit DNA virus-induced IRF3 phosphor-ylation (Figure S6F). Because NF-κB is involved in the induction of IFN and ISGs (Chen et al., 2016b; Pfeffer, 2011), it is possible that salicylic acid could partially inhibit DNA-induced IFN production and ISG expression by inhibiting NF-κB. Indeed, sal-icylic acid had an inhibitory effect on the expression of ISGs in
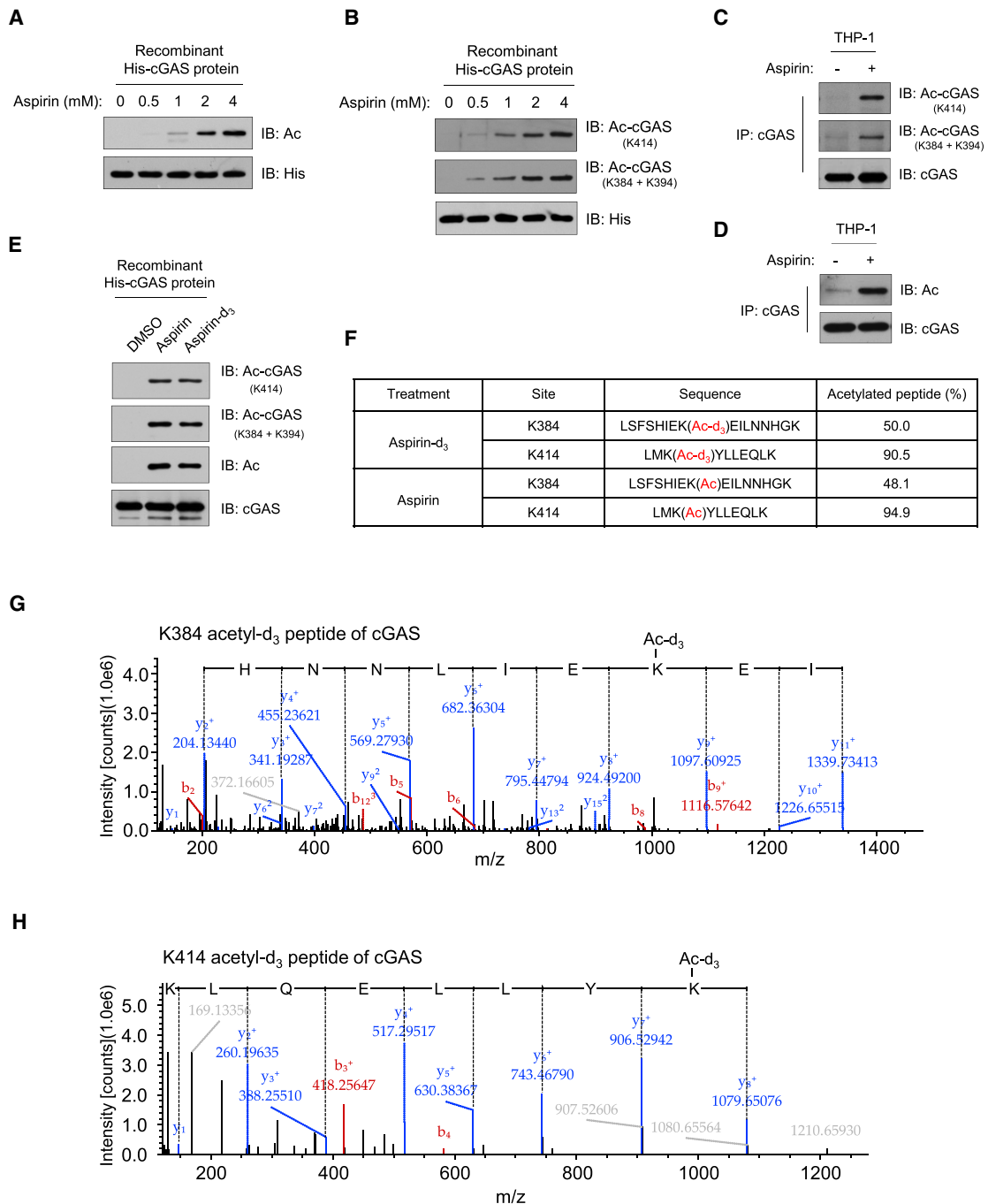
Cell

F

Treatment	Site	Sequence	Acetylated peptide (%)
Aspirin-d$_3$	K384	LSFSHIEK(Ac-d$_3$)EILNNHGK	50.0
	K414	LMK(Ac-d$_3$)YLLEQLK	90.5
Aspirin	K384	LSFSHIEK(Ac)EILNNHGK	48.1
	K414	LMK(Ac)YLLEQLK	94.9

G

H

Figure 4. Aspirin Directly Acetylates cGAS

(A and B) Incubation of recombinant cGAS protein with aspirin. Shown is immunoblot analysis of cGAS acetylation with a pan-acetyl-lysine antibody (A) or site-specific cGAS acetylation antibodies (B).

(C and D) PMA-differentiated THP-1 cells were treated with DMSO (−) or aspirin (4 mM) for 24 h, and cGAS was immunoprecipitated. cGAS acetylation was analyzed by immunoblotting with site-specific cGAS acetylation antibodies (C) or pan-acetyl-lysine antibody (D).

(E) Incubation of recombinant cGAS protein with aspirin (4 mM) or isotopically labeled aspirin-d$_3$ (4 mM). Shown is immunoblot analysis of cGAS acetylation with a pan-acetyl-lysine antibody or site-specific cGAS acetylation antibodies.

(F–H) PMA-differentiated FLAG-cGAS-expressing THP-1 cells were treated with aspirin-d$_3$ (4 mM) or aspirin (4 mM) for 24 h, and FLAG-cGAS was immuno-precipitated. The percentage of cGAS acetylation of the indicated sites (F) and the representative K384 (G) and K414 (H) acetylated peptides of cGAS with acetyl-d$_3$ were analyzed by Thermo Scientific Q Exactive HF Hybrid Quadrupole-Orbitrap mass spectrometer. The y ion peaks are shown in blue, and the b ion

(legend continued on next page)

Cell

Trex1$^{-/-}$ bone marrow cells (Figure S6G). However, compared with aspirin, this inhibitory effect was much weaker, especially in lower concentrations (Figures 6A and S6G). In line with these observations, after daily injection of these drugs for 1 week, we detected ISG expression levels in mouse hearts, a widely used indicator for disease phenotype (Gao et al., 2015; Gray et al., 2015), and found that, although aspirin significantly reduced ISG expression in the hearts of *Trex1*$^{-/-}$ mice, salicylic acid had a weak effect, and diclofenac sodium did not have any effect (Figure 6B). By detecting m-cGAS acetylation in spleens, which express much higher levels of m-cGAS than the hearts of these mice, we found that aspirin injection led to obviously increased m-cGAS acetylation in mouse tissue (Figure 6C). As expected, neither salicylic acid nor diclofenac sodium acetylated cGAS in mouse tissue (Figure 6C). We also detected m-cGAS acetylation in spleens from both wild-type and *Trex1*$^{-/-}$ mice. Consistent with our finding that DNA treatment led to the deacetylation of cGAS, our results showed that, in the spleens of *Trex1*$^{-/-}$ mice, m-cGAS acetylation levels were reduced (Figure S6H). Further, daily injection with aspirin, but not salicylic acid or diclofenac sodium, significantly prolonged the survival of *Trex1*$^{-/-}$ mice (Figure 6D). Thus, these data suggest that the inhibitory effect of aspirin is unlikely to be through inhibition of the COX-1/2 pathway and that acetylation is important for aspirin-mediated inhibition on self-DNA-induced autoimmunity.

Because we showed that HDAC3 mediated the deacetylation of cGAS in response to DNA, we next tested whether inhibiting HDAC3 could be effective in ameliorating the autoimmune phenotype in *Trex1*$^{-/-}$ mice. To do so, we first treated *Trex1* knockdown L929 cells with two HDAC inhibitors, RGFP966 and MS-275. RGFP966 is a selective inhibitor of HDAC3 (Malvaez et al., 2013), and MS-275 can target HDAC1 and HDAC3 (Tatamiya et al., 2004). By measuring the expression levels of ISGs in the treated cells, we found that, although RGFP966 had a mild inhibitory effect on ISG expression, MS-275 inhibited ISG efficiently (Figure S6I). These data are consistent with our original cell experiments showing that knockdown of HDAC3 only partially blocked cGAS activation (Figures 3E and S3E), which indicated that other deacetylases may also contribute to cGAS deacetylation. Given the strong inhibitory effect of MS-275 and that MS-275 is a drug approved by the Food and Drug Administration (FDA), we next used MS-275 to treat *Trex1*$^{-/-}$ mice. Our results showed that MS-275 can inhibit ISG levels in the hearts of *Trex1*$^{-/-}$ mice (Figure 6E). Thus, targeting HDAC could also have an inhibitory effect on self-DNA-induced autoimmune responses in *Trex1*$^{-/-}$ mice.

Aspirin Suppresses DNA-Mediated Autoimmunity in Human Patient Cells

To further study the effectiveness of aspirin in treating AGS, we recruited an AGS patient and his healthy elder brother from an AGS family (Guo et al., 2014) and isolated PBMCs from the brothers. We first confirmed the frameshift mutation

(c.459_460insA) of *TREX1* in the AGS sibling, whose PBMCs had very little TREX1 expression (Figures 7A and 7B) and highly elevated levels of ISGs (Figure 7C). Treatment of the AGS patient's PBMCs with aspirin significantly reduced the levels of ISGs (Figure 7C). MS-275 treatment also reduced the elevated ISG levels in patient cells (Figure S7A). Thus, our data further support the idea that aspirin could be used to treat self-DNA-induced autoimmune responses.

Aspirin Suppresses cGAS-Mediated Type I Interferonopathies

To determine whether aspirin-mediated cGAS inhibition presents a therapeutic strategy for other cGAS-related primary interferonopathies, we used small interfering RNAs (siRNAs) to knock down the expression of *Dnase2a* or *Rnaseh2b* in L929 cells. It has been reported previously that the loss-of-function mutations of *Dnase2a* or *Rnaseh2b* lead to type I interferonopathies (Crow and Manel, 2015; Gao et al., 2015; Mackenzie et al., 2016); deficiency of *Dnase2a* or *Rnaseh2b* resulted in significantly elevated ISG expression, and, importantly, elevated ISG expression was efficiently inhibited by aspirin (Figures S7B–S7E). STING-associated vasculopathy with onset in infancy (SAVI) is a recently characterized form of AGS-like disease caused by auto-activating mutations in STING (Liu et al., 2014; Melki et al., 2017). Because this disease affects a step downstream of cGAS activation, we tested whether aspirin has any effect in an SAVI model. To do so, we created a gain-of-function-mutated STING-driven cell model. We found that aspirin treatment had no effect on STING-mediated IRF3 phosphorylation, whereas BX-795, a known TBK1 inhibitor (Clark et al., 2009), strongly inhibited IRF3 phosphorylation (Figure S7F). These data indicate that aspirin only affects cGAS- but not STING-mediated immune responses.

DISCUSSION

Detection of cytosolic DNA by cGAS is critical for the immune system to sense and fight against infection. However, deregulated chronic activation of cGAS by self-DNA is the primary cause for several devastating autoimmune diseases, including lupus and AGS (Crow and Manel, 2015; Gao et al., 2015; Gray et al., 2015; Lisnevskaia et al., 2014; Mackenzie et al., 2016), but so far, there is no effective therapy for treating these diseases (Crow et al., 2015). In the current study, we report a novel regulation of cGAS activity. Our findings also indicate that aspirin could be used to inhibit cGAS activation and treat self-DNA-induced autoimmune diseases.

Aspirin is widely used to treat inflammation by inhibiting COX. In our study, using another specific COX inhibitor, diclofenac sodium, we found that diclofenac sodium had no effect on cGAS activation. This result suggests that aspirin-mediated inhibition of cGAS activation is not related to its effect on COX. It is known that cGAS activates downstream IRF3 and NF-κB signaling via

peaks are shown in red. The partial amino acid sequence (from left to right, C-terminal to N-terminal) deduced from y ions is shown on the spectrum. The mass difference between y$_9$ and y$_8$ ions (G) or y$_8$ and y$_7$ ions (H) is the mass of the acetyl-d3-modified lysine residue.
Anti-His blots (A and B) indicate loading of lanes. Data represent at least three independent experiments.
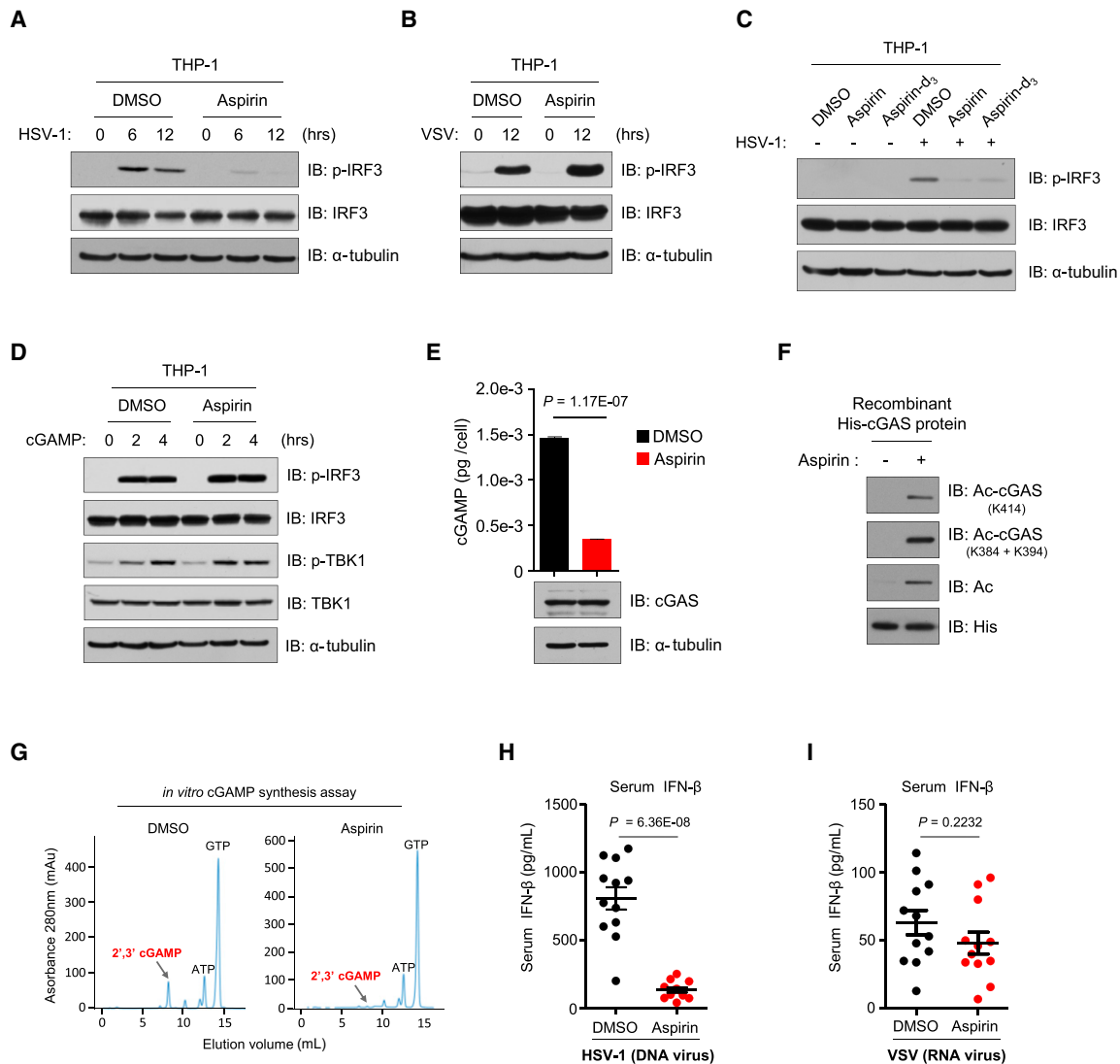See also Figure S4 and Table S2.

Figure 5. Aspirin Inhibits cGAS-Mediated IFN Production

(A and B) PMA-differentiated THP-1 cells were infected with HSV-1 (MOI = 10:1) (A) or VSV (MOI = 10:1) (B) after DMSO or aspirin (4 mM) pretreatment, and the phosphorylation of IRF3 was analyzed by immunoblotting.

(C) PMA-differentiated THP-1 cells were infected with HSV-1 (MOI = 10:1) after DMSO, aspirin (4 mM), or aspirin-d_3 (4 mM) pretreatment, and the phosphorylation of IRF3 was analyzed by immunoblotting.

(D) PMA-differentiated THP-1 cells were pre-treated with DMSO or aspirin (4 mM) for 24 h, followed by treatment with cGAMP (1 μg/mL) for the indicated hours. Shown is immunoblot analysis of the phosphorylation of IRF3 and TBK1.

(E) PMA-differentiated THP-1 cells were treated with DMSO or aspirin for 24 h, followed by a 2-h treatment of HT-DNA (1 μg/mL). cGAMP production was quantified by LC-MS/MRM; data are mean ± SEM from triplicates (technical replicates), unpaired t test. Shown is immunoblot analysis of cGAS in the corresponding protein samples (bottom).

(F and G) Immunoblot analysis (F) and *in vitro* cGAMP synthesis assay (G) of recombinant cGAS proteins in the presence of DMSO or aspirin (4 mM). Site-specific cGAS acetylation antibodies and the pan-acetyl-lysine antibody were used to analyze cGAS acetylation. The anti-His blot indicates loading of lanes (F).

(H and I) Wild-type C57BL/6J mice were given a daily intraperitoneal (i.p.) injection of DMSO (n = 12) or aspirin (50 mg/kg, n = 12) for 2 days, followed by i.p. injection of either HSV-1 (H) or VSV (I) for 6 h. Serum from mice was obtained for ELISA analysis of IFN-β concentration. Data are mean ± SEM, unpaired t test.

Anti-α-tubulin blots indicate loading of lanes (A–E). Combined data of two independent experiments are shown (H and I); other data represent three independent experiments.
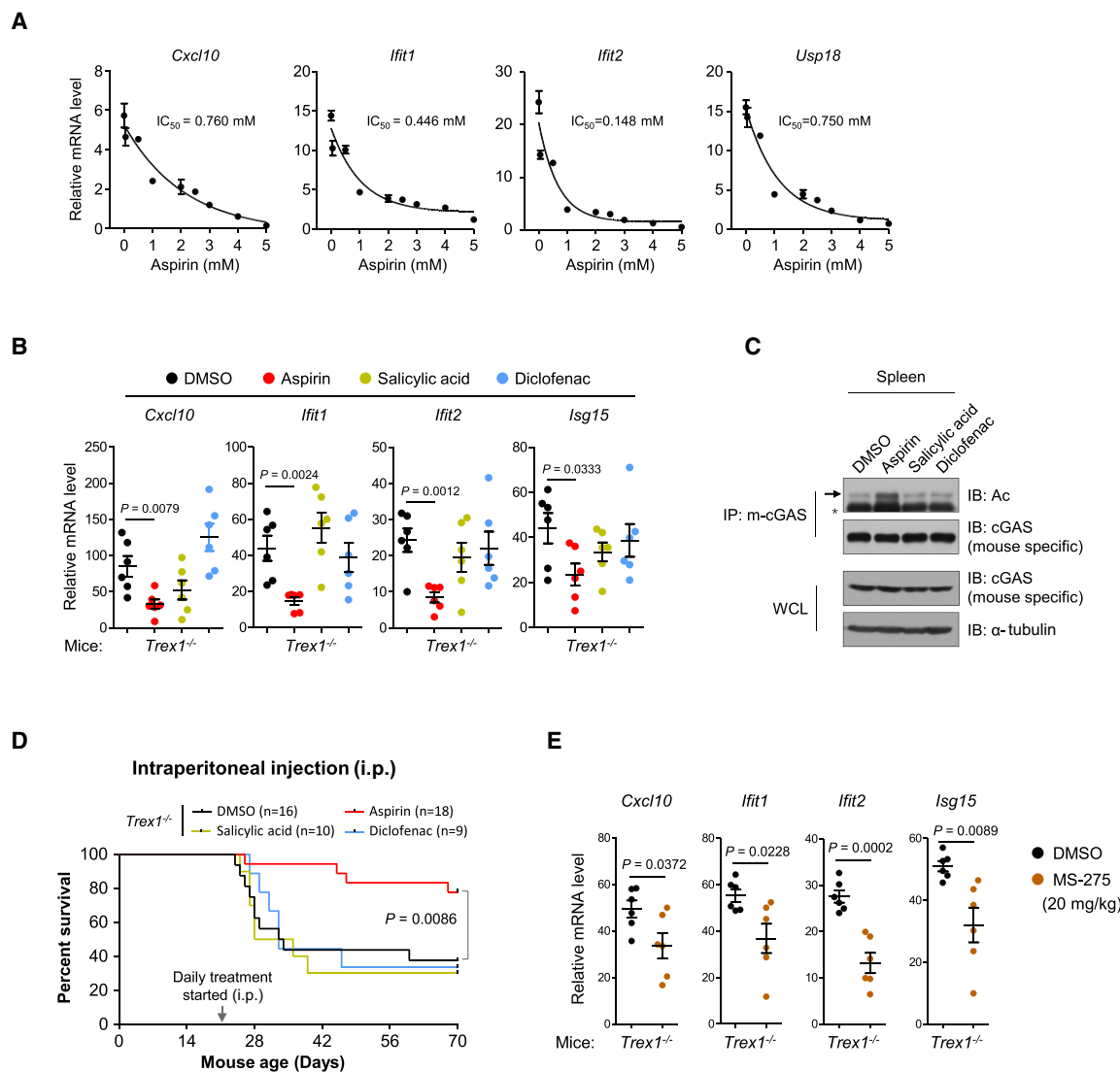
See also Figure S5.

Cell

Figure 6. Aspirin Suppresses DNA-Mediated Autoimmunity in Mice

(A) Bone marrow cells from $Trex1^{-/-}$ mice were treated with aspirin at the indicated concentrations for 2 days. The mRNA levels of ISGs, as indicated, were analyzed by qPCR (relative to that of WT bone marrow cells). The IC_{50} was calculated by Statistical Package for the Social Sciences (SPSS). Data are mean ± SEM from triplicates (technical replicates).

(B) $Trex1^{-/-}$ mice (n = 6) were given daily administration (i.p.) of aspirin (50 mg/kg), salicylic acid (50 mg/kg), diclofenac sodium (1 mg/kg), or DMSO for 7 days, and then the mRNA levels of ISGs in the mouse hearts were analyzed by qPCR. Data are mean ± SEM, unpaired t test.

(C) 3-week old $Trex1^{-/-}$ mice were given daily treatment of aspirin (50 mg/kg), salicylic acid (50 mg/kg), diclofenac sodium (1 mg/kg), or DMSO for 1 week by i.p. injection. m-cGAS in the spleen was immunoprecipitated, and the acetylation of m-cGAS was analyzed with pan-acetyl-lysine antibody; anti-α-tubulin blots indicate loading of lanes. * indicates non-specific bands.

(D) 3-week old $Trex1^{-/-}$ mice were administered (i.p.) aspirin (50 mg/kg), salicylic acid (50 mg/kg), diclofenac sodium (1 mg/kg), or DMSO daily. Survival curves of mice are shown. Statistical analysis was performed with a log rank (Mantel-Cox) test.

(E) $Trex1^{-/-}$ mice (n = 6) were given daily administration (i.p.) of MS-275 (20 mg/kg) or DMSO for 10 days, mRNA levels of ISGs in mouse hearts were analyzed by qPCR. Data are mean ± SEM, unpaired t test.

Data represent at least two independent experiments (A–C and E); combined data of at least two independent experiments are shown (D).

See also Figure S6.

STING (Sun et al., 2013) and that both IRF3 and NF-κB are involved in the production of IFN (Chen et al., 2016b). It has also been reported that NF-κB can regulate the expression of some ISGs (Pfeffer, 2011). As expected, salicylic acid had a partial inhibitory effect on ISG expression, possibly through inhibition of the NF-κB pathway. In contrast to salicylic acid, however, aspirin may inhibit the activation of both IRF3 and NF-κB by targeting cGAS. Therefore, aspirin, but not salicylic acid,
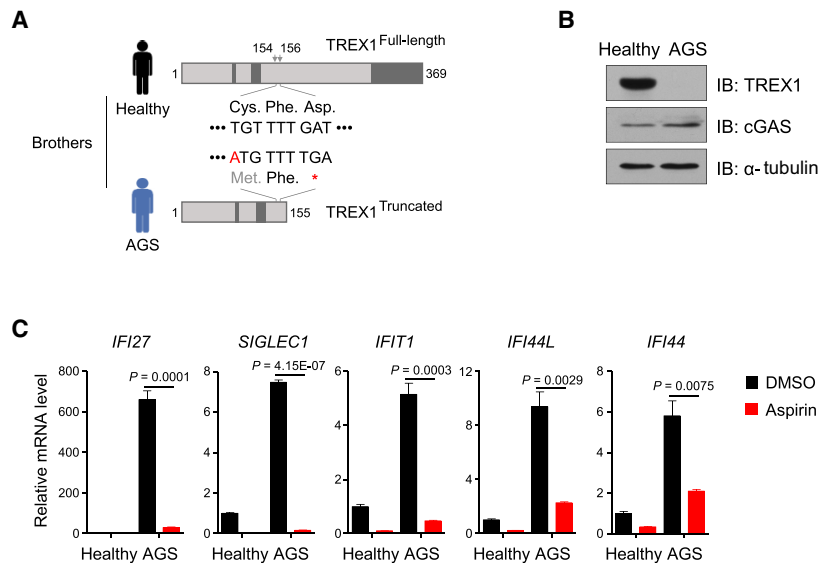
Cell

Figure 7. Aspirin Suppresses DNA-Mediated Autoimmunity in Human Patient Cells

(A) Schematic diagram showing the frameshift mutation of *TREX1* in the AGS patient (AGS, bottom) in comparison with his healthy brother (Healthy, top). The frameshift mutation (c. 459-460insA, red A in the diagram) results in a premature stop codon (red *) at the position of the 156th amino acid. The dark gray color in the schematic indicates different regions according to Uniprot: Q9NSU2-1. The first region (position 75–76) is described as a substrate-binding region, the second region (position 109–118) is a proline-rich region, and the last region (position 291–369) is necessary for endoplasmic reticulum localization.

(B) Immunoblot analysis of TREX1 and cGAS in PBMCs from the healthy brother and the AGS patient; the anti-α-tubulin blot indicates loading of lanes.

(C) PBMCs from the healthy brother and the AGS patient were treated with DMSO or aspirin (4 mM) for 2 days. The mRNA levels of ISGs were detected by qPCR. Data are mean ± SEM from triplicates (technical replicates), unpaired t test.

Data represent at least two independent experiments (B and C).

See also Figure S7.

was effective in promoting the survival of $Trex1^{-/-}$ mice. Moreover, using isotopically labeled aspirin, we demonstrated direct acetylation of cGAS by aspirin. Our findings collectively suggest that aspirin functions as a tangible cGAS inhibitor.

Aspirin has been shown to acetylate many protein targets in addition to cGAS. It is possible that aspirin also targets other proteins in addition to cGAS *in vivo*. However, we showed that aspirin strongly inhibited cGAS-mediated TBK1-IRF3 signaling but did not affect STING activator cGAMP- or c-di-GMP-induced downstream TBK1-IRF3 signaling. We also showed that aspirin did not inhibit SAVI-associated STING mutant-mediated IRF3 activation. In addition, aspirin only had a marginal effect on RNA virus-induced IFN production in mice. These data indicate that the inhibitory effect of aspirin on the DNA-cGAS-STING-TBK1-IRF3 axis is mainly achieved through inhibition of cGAS.

With an acetyl-lysine-incorporating protein synthesis system, we generated recombinant acetylated cGAS proteins and showed that the acetylation on these residues strongly inhibits the activity of cGAS. It has been reported that these acetylation sites are involved in the DNA binding of cGAS (Civril et al., 2013; Gao et al., 2013; Kranzusch et al., 2013; Zhang et al., 2014; Zhou et al., 2018). Using recombinant acetylated cGAS proteins, we found that the acetylation on each of the individual sites slightly reduced the DNA binding activity of cGAS. These data are consistent with a previous study showing that the mutations on some of these residues have only a limited effect on DNA binding of cGAS (Li et al., 2013). Accumulating evidence suggests that several regions of cGAS protein are important for cGAS-DNA binding (Civril et al., 2013; Gao et al., 2013; Kranzusch et al., 2013; Li et al., 2013; Zhang et al., 2014; Zhou et al., 2018). Therefore, when K384, K394, or K414 is acetylated, other regions of cGAS, such as the N-terminal region (Du and Chen, 2018; Lee et al., 2017; Tao et al., 2017), could still contribute to DNA binding. Binding of DNA to cGAS led to deacetylation of cGAS, promoting cGAS activation.

Our study suggests that K414 is a critical residue for cGAS function. Interestingly, a recent study reported that, in resting cells, cGAS undergoes K48-linked ubiquitination at K414, leading to p62-dependent selective autophagic degradation of cGAS and that, upon DNA virus infection, this inhibitory ubiquitination is removed to promote cGAS activation (Chen et al., 2016a). It is likely that, on K414, acetylation may compete with ubiquitination to maintain a proper level of cGAS protein in resting cells. K27-linked ubiquitination on K384 of cGAS has been shown to potentiate cGAS activity in response to DNA virus infection (Wang et al., 2017). In response to DNA treatment, HDAC-mediated removal of K384 acetylation may allow the K27-linked ubiquitination on K384 to further promote cGAS activation. Together, K384 and K414 of cGAS are critical residues for cGAS regulation by multiple PTMs. Future studies are necessary to further investigate the complex interplay of these PTMs.

The deletion of *Cgas* eliminated the lethality and autoimmune phenotypes in $Trex1^{-/-}$ mice, emphasizing the importance of cGAS inhibition in treating these diseases (Gao et al., 2015; Gray et al., 2015). cGAS has been shown to be regulated by phosphorylation, glutamylation, and sumoylation (Hu et al., 2016; Seo et al., 2015; Xia et al., 2016), but further efforts are needed to develop chemicals that can alter these modifications on cGAS to inhibit its activity. Screening of cGAS inhibitors based on the cGAS crystal structure has been reported recently, but none of these inhibitors have been tested in mouse AGS models or human AGS patients (An et al., 2015). In this study, we revealed that acetylation inhibits cGAS activity. This regulation of cGAS seems to be evolutionarily conserved because the acetylation sites we identified are conserved across species. More importantly, we demonstrated that a commonly used NSAID, aspirin, could inhibit cGAS activation through acetylation and be used to treat AGS and potentially other DNA-mediated autoimmune diseases. Particularly, the effective dosage of aspirin needed for inhibiting cGAS falls well below the upper limit

Cell

for its use in humans. Therefore, our findings provide a feasible therapy for treating AGS and other autoimmune diseases.

STAR★METHODS

Detailed methods are provided in the online version of this paper and include the following:

- KEY RESOURCES TABLE
- CONTACT FOR REAGENT AND RESOURCE SHARING
- EXPERIMENTAL MODELS AND SUBJECT DETAILS
  - ○ Mice
  - ○ Cells
  - ○ Viruses
- METHODS DETAILS
  - ○ Quantitative Polymerase Chain Reaction (qPCR)
  - ○ ELISA
  - ○ Isolation of PBMCs from AGS patient
  - ○ Mass Spectrometry
  - ○ Immunoblotting and Immunoprecipitation
  - ○ Purification of site-specific acetylated cGAS recombinant proteins
  - ○ *In vitro* cGAMP synthesis assay
  - ○ cGAMP extraction
  - ○ Quantification of cGAMP using LC–MS/MRM
  - ○ RNA Interference
  - ○ IC_{50} Determination
  - ○ DNA Binding Assay
  - ○ Immunofluorescence
  - ○ cGAS dimerization
- QUANTIFICATION AND STATISTICAL ANALYSIS
- DATA AND SOFTWARE AVAILABILITY

SUPPLEMENTAL INFORMATION

Supplemental Information includes seven figures and three tables and can be found with this article online at https://doi.org/10.1016/j.cell.2019.01.016.

AUTHOR CONTRIBUTIONS

Tao Li and X.-M.Z. supervised the project. Tao Li, J.D., Y.-J.H., and X.H. designed the experiments. Y.-J.H., X.H., M.Z., H.C., S.-Y.H., N.S., X.D., J.M., and Y.C. performed the mouse studies and experiments in cells. J.D., H.W., K.H., W.-H.L., and X.W. performed mass spectrometry analysis for cGAS acetylation and cGAS-interacting proteins. J.D., Z.S., J.-H.M., and Z.-S.L. per-

formed the *in vitro* cGAMP synthesis assay. Y.-J.H., M.Z., N.W., W.X., Tingting Li, Q.-Y.H., and X.-Y.Z. performed cGAMP detection by LC-MS/MRM. J.D., Y.-J.H., A.-L.L., T.Z., and Tao Li analyzed the data. Tao Li, Z.-G.L., and X.-M.Z. wrote the manuscript.

REFERENCES

Ahn, J., and Barber, G.N. (2014). Self-DNA, STING-dependent signaling and the origins of autoinflammatory disease. Curr. Opin. Immunol. *31*, 121–126.

Aicardi, J., and Goutières, F. (1984). A progressive familial encephalopathy in infancy with calcifications of the basal ganglia and chronic cerebrospinal fluid lymphocytosis. Ann. Neurol. *15*, 49–54.

An, J., Woodward, J.J., Sasaki, T., Minie, M., and Elkon, K.B. (2015). Cutting edge: Antimalarial drugs inhibit IFN-β production through blockade of cyclic GMP-AMP synthase-DNA interaction. J. Immunol. *194*, 4089–4093.

Barbalat, R., Ewald, S.E., Mouchess, M.L., and Barton, G.M. (2011). Nucleic acid recognition by the innate immune system. Annu. Rev. Immunol. *29*, 185–214.

Bowie, A. (2012). The STING in the tail for cytosolic DNA-dependent activation of IRF3. Sci. Signal. *5*, pe9.

Burdette, D.L., Monroe, K.M., Sotelo-Troha, K., Iwig, J.S., Eckert, B., Hyodo, M., Hayakawa, Y., and Vance, R.E. (2011). STING is a direct innate immune sensor of cyclic di-GMP. Nature *478*, 515–518.

Charifson, P.S., and Walters, W.P. (2014). Acidic and basic drugs in medicinal chemistry: a perspective. J. Med. Chem. *57*, 9701–9717.

Chen, M., Meng, Q., Qin, Y., Liang, P., Tan, P., He, L., Zhou, Y., Chen, Y., Huang, J., Wang, R.F., and Cui, J. (2016a). TRIM14 Inhibits cGAS Degradation Mediated by Selective Autophagy Receptor p62 to Promote Innate Immune Responses. Mol. Cell *64*, 105–119.

Chen, Q., Sun, L., and Chen, Z.J. (2016b). Regulation and function of the cGAS-STING pathway of cytosolic DNA sensing. Nat. Immunol. *17*, 1142–1149.

Choudhary, C., Kumar, C., Gnad, F., Nielsen, M.L., Rehman, M., Walther, T.C., Olsen, J.V., and Mann, M. (2009). Lysine acetylation targets protein complexes and co-regulates major cellular functions. Science *325*, 834–840.

Civril, F., Deimling, T., de Oliveira Mann, C.C., Ablasser, A., Moldt, M., Witte, G., Hornung, V., and Hopfner, K.P. (2013). Structural mechanism of cytosolic DNA sensing by cGAS. Nature *498*, 332–337.

Clark, K., Plater, L., Peggie, M., and Cohen, P. (2009). Use of the pharmacological inhibitor BX795 to study the regulation and physiological roles of TBK1 and IkappaB kinase epsilon: a distinct upstream kinase mediates Ser-172 phosphorylation and activation. J. Biol. Chem. *284*, 14136–14146.

Cohen, P. (2000). The regulation of protein function by multisite phosphorylation–a 25 year update. Trends Biochem. Sci. *25*, 596–601.

Crow, Y.J., and Manel, N. (2015). Aicardi-Goutières syndrome and the type I interferonopathies. Nat. Rev. Immunol. *15*, 429–440.

Crow, Y.J., Hayward, B.E., Parmar, R., Robins, P., Leitch, A., Ali, M., Black, D.N., van Bokhoven, H., Brunner, H.G., Hamel, B.C., et al. (2006). Mutations in the gene encoding the 3′-5′ DNA exonuclease TREX1 cause Aicardi-Goutières syndrome at the AGS1 locus. Nat. Genet. *38*, 917–920.

Crow, Y.J., Chase, D.S., Lowenstein Schmidt, J., Szynkiewicz, M., Forte, G.M., Gornall, H.L., Oojageer, A., Anderson, B., Pizzino, A., Helman, G., et al. (2015). Characterization of human disease phenotypes associated with mutations in TREX1, RNASEH2A, RNASEH2B, RNASEH2C, SAMHD1, ADAR, and IFIH1. Am. J. Med. Genet. A. *167A*, 296–312.

di Palma, A., Matarese, G., Leone, V., Di Matola, T., Acquaviva, F., Acquaviva, A.M., and Ricchi, P. (2006). Aspirin reduces the outcome of anticancer therapy in Meth A-bearing mice through activation of AKT-glycogen synthase kinase signaling. Mol. Cancer Ther. 5, 1318–1324.

Du, M., and Chen, Z.J. (2018). DNA-induced liquid phase condensation of cGAS activates innate immune signaling. Science 361, 704–709.

Elkon, K.B., and Wiedeman, A. (2012). Type I IFN system in the development and manifestations of SLE. Curr. Opin. Rheumatol. 24, 499–505.

Gao, P., Ascano, M., Wu, Y., Barchet, W., Gaffney, B.L., Zillinger, T., Serganov, A.A., Liu, Y., Jones, R.A., Hartmann, G., et al. (2013). Cyclic [G(2′,5′)pA(3′,5′)p] is the metazoan second messenger produced by DNA-activated cyclic GMP-AMP synthase. Cell 153, 1094–1107.

Gao, D., Li, T., Li, X.D., Chen, X., Li, Q.Z., Wight-Carter, M., and Chen, Z.J. (2015). Activation of cyclic GMP-AMP synthase by self-DNA causes autoimmune diseases. Proc. Natl. Acad. Sci. USA 112, E5699–E5705.

Grabocka, E., and Bar-Sagi, D. (2016). Mutant KRAS Enhances Tumor Cell Fitness by Upregulating Stress Granules. Cell 167, 1803–1813.e1812.

Gray, E.E., Treuting, P.M., Woodward, J.J., and Stetson, D.B. (2015). Cutting Edge: cGAS Is Required for Lethal Autoimmune Disease in the Trex1-Deficient Mouse Model of Aicardi-Goutières Syndrome. J. Immunol. 195, 1939–1943.

Guo, H., Li, C., Wang, M., Mao, N., Wang, S., Chang, G., and Cao, B. (2014). Clinicopathological and genetic analysis of Aicardi-Goutieres syndrome. Chin. J. Neurol. 47, 96–100.

Hu, M.M., Yang, Q., Xie, X.Q., Liao, C.Y., Lin, H., Liu, T.T., Yin, L., and Shu, H.B. (2016). Sumoylation Promotes the Stability of the DNA Sensor cGAS and the Adaptor STING to Regulate the Kinetics of Response to DNA Virus. Immunity 45, 555–569.

Hutt, A.J., Caldwell, J., and Smith, R.L. (1986). The metabolism of aspirin in man: a population study. Xenobiotica 16, 239–249.

Ishikawa, H., and Barber, G.N. (2008). STING is an endoplasmic reticulum adaptor that facilitates innate immune signalling. Nature 455, 674–678.

Jin, L., Waterman, P.M., Jonscher, K.R., Short, C.M., Reisdorph, N.A., and Cambier, J.C. (2008). MPYS, a novel membrane tetraspanner, is associated with major histocompatibility complex class II and mediates transduction of apoptotic signals. Mol. Cell. Biol. 28, 5014–5026.

Kassiotis, G., and Stoye, J.P. (2016). Immune responses to endogenous retroelements: taking the bad with the good. Nat. Rev. Immunol. 16, 207–219.

Kopp, E., and Ghosh, S. (1994). Inhibition of NF-kappa B by sodium salicylate and aspirin. Science 265, 956–959.

Kranzusch, P.J., Lee, A.S., Berger, J.M., and Doudna, J.A. (2013). Structure of human cGAS reveals a conserved family of second-messenger enzymes in innate immunity. Cell Rep. 3, 1362–1368.

Lee, A., Park, E.B., Lee, J., Choi, B.S., and Kang, S.J. (2017). The N terminus of cGAS de-oligomerizes the cGAS:DNA complex and lifts the DNA size restriction of core-cGAS activity. FEBS Lett. 591, 954–961.

Li, X., Shu, C., Yi, G., Chaton, C.T., Shelton, C.L., Diao, J., Zuo, X., Kao, C.C., Herr, A.B., and Li, P. (2013). Cyclic GMP-AMP synthase is activated by double-stranded DNA-induced oligomerization. Immunity 39, 1019–1031.

Lisnevskaia, L., Murphy, G., and Isenberg, D. (2014). Systemic lupus erythematosus. Lancet 384, 1878–1888.

Liu, Y., Jesus, A.A., Marrero, B., Yang, D., Ramsey, S.E., Sanchez, G.A.M., Tenbrock, K., Wittkowski, H., Jones, O.Y., Kuehn, H.S., et al. (2014). Activated STING in a vascular and pulmonary syndrome. N. Engl. J. Med. 371, 507–518.

Mackenzie, K.J., Carroll, P., Lettice, L., Tarnauskaitė, Ž., Reddy, K., Dix, F., Revuelta, A., Abbondati, E., Rigby, R.E., Rabe, B., et al. (2016). Ribonuclease H2 mutations induce a cGAS/STING-dependent innate immune response. EMBO J. 35, 831–844.

Malvaez, M., McQuown, S.C., Rogge, G.A., Astarabadi, M., Jacques, V., Carreiro, S., Rusche, J.R., and Wood, M.A. (2013). HDAC3-selective inhibitor enhances extinction of cocaine-seeking behavior in a persistent manner. Proc. Natl. Acad. Sci. USA 110, 2647–2652.

Melki, I., Rose, Y., Uggenti, C., Van Eyck, L., Frémond, M.L., Kitabayashi, N., Rice, G.I., Jenkinson, E.M., Boulai, A., Jeremiah, N., et al. (2017). Disease-associated mutations identify a novel region in human STING necessary for the control of type I interferon signaling. J. Allergy Clin. Immunol. 140, 543–552.e5.

Morita, M., Stamp, G., Robins, P., Dulic, A., Rosewell, I., Hrivnak, G., Daly, G., Lindahl, T., and Barnes, D.E. (2004). Gene-targeted mice lacking the Trex1 (DNase III) 3′−>5′ DNA exonuclease develop inflammatory myocarditis. Mol. Cell. Biol. 24, 6719–6727.

Neumann, H., Peak-Chew, S.Y., and Chin, J.W. (2008). Genetically encoding N(epsilon)-acetyllysine in recombinant proteins. Nat. Chem. Biol. 4, 232–234.

O'Neill, L.A. (2013). Immunology. Sensing the dark side of DNA. Science 339, 763–764.

Pfeffer, L.M. (2011). The role of nuclear factor kappaB in the interferon response. J. Interferon Cytokine Res. 31, 553–559.

Roth, G.J., and Majerus, P.W. (1975). The mechanism of the effect of aspirin on human platelets. I. Acetylation of a particulate fraction protein. J. Clin. Invest. 56, 624–632.

Seo, G.J., Yang, A., Tan, B., Kim, S., Liang, Q., Choi, Y., Yuan, W., Feng, P., Park, H.S., and Jung, J.U. (2015). Akt Kinase-Mediated Checkpoint of cGAS DNA Sensing Pathway. Cell Rep. 13, 440–449.

Shakespear, M.R., Halili, M.A., Irvine, K.M., Fairlie, D.P., and Sweet, M.J. (2011). Histone deacetylases as regulators of inflammation and immunity. Trends Immunol. 32, 335–343.

Stetson, D.B., Ko, J.S., Heidmann, T., and Medzhitov, R. (2008). Trex1 prevents cell-intrinsic initiation of autoimmunity. Cell 134, 587–598.

Sun, W., Li, Y., Chen, L., Chen, H., You, F., Zhou, X., Zhou, Y., Zhai, Z., Chen, D., and Jiang, Z. (2009). ERIS, an endoplasmic reticulum IFN stimulator, activates innate immune signaling through dimerization. Proc. Natl. Acad. Sci. USA 106, 8653–8658.

Sun, L., Wu, J., Du, F., Chen, X., and Chen, Z.J. (2013). Cyclic GMP-AMP synthase is a cytosolic DNA sensor that activates the type I interferon pathway. Science 339, 786–791.

Tao, J., Zhang, X.W., Jin, J., Du, X.X., Lian, T., Yang, J., Zhou, X., Jiang, Z., and Su, X.D. (2017). Nonspecific DNA Binding of cGAS N Terminus Promotes cGAS Activation. J. Immunol. 198, 3627–3636.

Tatamiya, T., Saito, A., Sugawara, T., and Nakanishi, O. (2004). Isozyme-selective activity of the HDAC inhibitor MS-275. Cancer Res. 64, 567.

Tatham, M.H., Cole, C., Scullion, P., Wilkie, R., Westwood, N.J., Stark, L.A., and Hay, R.T. (2017). A Proteomic Approach to Analyze the Aspirin-mediated Lysine Acetylome. Mol. Cell. Proteomics 16, 310–326.

Vane, J.R., and Botting, R.M. (2003). The mechanism of action of aspirin. Thromb. Res. 110, 255–258.

Verdin, E., and Ott, M. (2015). 50 years of protein acetylation: from gene regulation to metabolism and beyond. Nat. Rev. Mol. Cell Biol. 16, 258–264.

Wang, H., Gau, B., Slade, W.O., Juergens, M., Li, P., and Hicks, L.M. (2014). The global phosphoproteome of Chlamydomonas reinhardtii reveals complex organellar phosphorylation in the flagella and thylakoid membrane. Mol. Cell. Proteomics 13, 2337–2353.

Wang, Q., Huang, L., Hong, Z., Lv, Z., Mao, Z., Tang, Y., Kong, X., Li, S., Cui, Y., Liu, H., et al. (2017). The E3 ubiquitin ligase RNF185 facilitates the cGAS-mediated innate immune response. PLoS Pathog. 13, e1006264.

Wu, C., Cheng, Y.Y., Yin, H., Song, X.N., Li, W.W., Zhou, X.X., Zhao, L.P., Tian, L.J., Han, J.C., and Yu, H.Q. (2013a). Oxygen promotes biofilm formation of Shewanella putrefaciens CN32 through a diguanylate cyclase and an adhesin. Sci. Rep. 3, 1945.

Wu, J., Sun, L., Chen, X., Du, F., Shi, H., Chen, C., and Chen, Z.J. (2013b). Cyclic GMP-AMP is an endogenous second messenger in innate immune signaling by cytosolic DNA. Science 339, 826–830.

Cell

Xia, P., Ye, B., Wang, S., Zhu, X., Du, Y., Xiong, Z., Tian, Y., and Fan, Z. (2016). Glutamylation of the DNA sensor cGAS regulates its binding and synthase activity in antiviral immunity. Nat. Immunol. 17, 369–378.

Yang, Y.G., Lindahl, T., and Barnes, D.E. (2007). Trex1 exonuclease degrades ssDNA to prevent chronic checkpoint activation and autoimmune disease. Cell 131, 873–886.

Yin, M.J., Yamamoto, Y., and Gaynor, R.B. (1998). The anti-inflammatory agents aspirin and salicylate inhibit the activity of I(kappa)B kinase-beta. Nature 396, 77–80.

Yuan, Z.L., Guan, Y.J., Chatterjee, D., and Chin, Y.E. (2005). Stat3 dimerization regulated by reversible acetylation of a single lysine residue. Science 307, 269–273.

Zhang, X., Wu, J., Du, F., Xu, H., Sun, L., Chen, Z., Brautigam, C.A., Zhang, X., and Chen, Z.J. (2014). The cytosolic DNA sensor cGAS forms an oligomeric complex with DNA and undergoes switch-like conformational changes in the activation loop. Cell Rep. 6, 421–430.

Zhao, S., Xu, W., Jiang, W., Yu, W., Lin, Y., Zhang, T., Yao, J., Zhou, L., Zeng, Y., Li, H., et al. (2010). Regulation of cellular metabolism by protein lysine acetylation. Science 327, 1000–1004.

Zhong, B., Yang, Y., Li, S., Wang, Y.Y., Li, Y., Diao, F., Lei, C., He, X., Zhang, L., Tien, P., and Shu, H.B. (2008). The adaptor protein MITA links virus-sensing receptors to IRF3 transcription factor activation. Immunity 29, 538–550.

Zhou, W., Whiteley, A.T., de Oliveira Mann, C.C., Morehouse, B.R., Nowak, R.P., Fischer, E.S., Gray, N.S., Mekalanos, J.J., and Kranzusch, P.J. (2018). Structure of the Human cGAS-DNA Complex Reveals Enhanced Control of Immune Surveillance. Cell 174, 300–311.e11.

Cell

STAR★METHODS

KEY RESOURCES TABLE

REAGENT or RESOURCE	SOURCE	IDENTIFIER
Antibodies		
Rabbit monoclonal anti-phospho-TBK1/NAK (Ser172)	Cell Signaling Technology	Cat# 5483P; RRID: AB_10693472
Rabbit monoclonal anti-TBK1	Cell Signaling Technology	Cat# 3504S; RRID: AB_2255663
Rabbit monoclonal anti-cGAS (mouse specific)	Cell Signaling Technology	Cat# 31659
Rabbit monoclonal anti-cGAS	Cell Signaling Technology	Cat# 15102; RRID: AB_2732795
Rabbit polyclonal anti-Acetylated-Lysine	Cell Signaling Technology	Cat 9441; RRID: AB_331805
Mouse monoclonal anti-Acetylated-Lysine	Cell Signaling Technology	Cat# 9681S; RRID: AB_331799
Mouse monoclonal anti-α-tubulin	Sigma-Aldrich	Cat# T5168; RRID: AB_477579
Mouse monoclonal anti-FLAG	Sigma-Aldrich	Cat# F3165; RRID: AB_259529
Rabbit monoclonal anti-HDAC3	Abcam	Cat# ab32369; RRID: AB_732780
Rabbit monoclonal anti-IRF3 (phospho S386)	Abcam	Cat# ab76493; RRID: AB_1523836
Rabbit monoclonal anti-IRF3	Abcam	Cat# ab68481; RRID: AB_11155653
Mouse monoclonal anti-TREX-1	Santa Cruz Biotechnology	Cat# sc-271870; RRID: AB_10708266
Mouse monoclonal anti-β-Actin	Santa Cruz Biotechnology	Cat# sc-47778; RRID: AB_626632
Rabbit polyclonal anti-HA-probe	Santa Cruz Biotechnology	Cat# sc-805; RRID: AB_631618
Mouse monoclonal anti-HDAC3	Santa Cruz Biotechnology	Cat# sc-376957; RRID: AB_2715509
Rabbit polyclonal anti-His-tag	MEDICAL & BIOLOGICAL LABORATORIES	Cat# PM032; RRID: AB_10209426
Rabbit polyclonal anti-cGAS	This paper	N/A
Rabbit polyclonal anti-Ac-cGAS (K384+K394)	This paper	N/A
Rabbit polyclonal anti-Ac-cGAS (K414)	This paper	N/A
Bacterial and Virus Strains		
HSV-1	Prof. Jiahuai Han (Xiamen U. China)	N/A
VSV	Prof. Hui Zhong (Molecular Genetics Department Beijing Institute of Biotechnology, China)	N/A
Chemicals, Peptides, and Recombinant Proteins		
Phorbol-12-myristate-13-acetate (PMA)	Merck	Cat# 524400; CAS No.16561-29-8
ATP Solution (100 mM)	ThermoFisher Scientific	Cat# R0441
GTP Solution (100 mM)	ThermoFisher Scientific	Cat# R0461
TRIzol	Thermo Fisher Scientific	Cat 15596018
Nε-Acetyl-L-lysine	Sigma-Aldrich	Cat# A4021; CAS No.692-04-6
HT-DNA	Sigma-Aldrich	Cat# D6898
Poly(I:C)	Sigma-Aldrich	Cat# P1530
Nicotinamide	Sigma-Aldrich	Cat# N0636; CAS No.98-92-0
Hexadimethrine bromide (Polybrene)	Sigma-Aldrich	Cat# H9268; CAS No. 28728-55-4
Histopaque®-1077	Sigma-Aldrich	Cat# 10771
Puromycin hydrochloride	Amresco	Cat# J593-25MG; CAS No.58-58-2
2′3′-cGAMP	Invivogen	Cat# tlrl-cga23
c-di-GMP	Invivogen	Cat# tlrl-cdg
Recombinant Human TNF-alpha Protein	R&D System	Cat# 210-TA
Trichostatin A (TSA)	Cell Signaling Technology	Cat# 9950S; CAS No.58880-19-6
Cycloheximide (CHX)	Cell Signaling Technology	Cat# 2112S; CAS No. 66-81-9

(Continued on next page)

Cell

Continued

REAGENT or RESOURCE	SOURCE	IDENTIFIER
Aspirin	Ouhe Technology	Cat# 50-78-2; CAS No.50-78-2
Aspirin-d3	Santa Cruz Biotechnology	Cat# sc-480464; CAS No.921943-73-9
Salicylic acid	Alfa Aesar	Cat# 30782; CAS No. 69-72-7
Diclofenac sodium	Aladdin	Cat# D129332; CAS No. 15307-79-6
MS-275	MedChemExpress	Cat# HY-12163; CAS No. 209783-80-2
RGFP966	Selleck	Cat# S7229; CAS No. 1396841-57-8
BX-795	Selleck	Cat# S1274; CAS No. 702675-74-9
Ni-NTA Agarose beads	QIAGEN	Mat. No. 1018244
Critical Commercial Assays		
IFN-β ELISA kit	Biolegend	Cat# 439408
Human PGE2 ELISA Kit	FineTest	Cat# EH4233
Experimental Models: Cell Lines		
Human: HEK293T	ATCC	Cat# CRL-11268
Human: THP-1	ATCC	Cat# TIB-202
Human: Human primary PBMCs	This paper	N/A
Human: HeLa	ATCC	Cat# CCL-2
Mouse: L929	ATCC	Cat# CCL-1
Experimental Models: Organisms/Strains		
Mouse: $Trex1^{+/-}$ C57BL/6J	Morita et al., 2004	N/A
Oligonucleotides		
Human cGAS-targeted sgRNA: CACCGAAGT GCGACTCCGCGTTCAG, AAACCTGAACGCG GAGTCGCACTTC	This paper	N/A
Biotinylated interferon stimulatory DNA: sense: 5′-Biotin-TACAGATCTACTAGTGATCTATGAC TGATCTGTACATGATCTACA-3′, anti-sense: 5′-TGTAGATCATGTACAGATCAGTCATAGAT CACTAGTAGATCTGTA-3′	Thermo Fisher Scientific	N/A
siRNA: mouse Trex1	Invitrogen	Cat#: MSS238570
siRNA: human HDAC3	RiboBio	Cat#: siB1032283530
siRNA: mouse Dnase2a	RiboBio	Cat#: siG151201033118
siRNA: mouse Rnaseh2b	RiboBio	Cat#: siG170516091413
qPCR pimers, see Table S3	This paper	N/A
Recombinant DNA		
pAcKRS-3	Prof. Jason W. Chin (Cambridge, UK)	N/A
pCDF PylT-1	Prof. Jason W. Chin (Cambridge, UK)	N/A
Human cGAS cDNA construct	Prof. Jea U. Jung (USC, USA)	N/A
Mouse Cgas cDNA construct	Prof.Russell E. Vance (UC Berkeley, USA)	N/A
STING cDNA construct	Prof. Hongbing Shu (Wuhan U, China)	N/A
lentiCRISPR v2	Addgene	Plasmid #52961
Software and Algorithms		
GraphPad Prism 5.0	GraphPad Software	https://www.graphpad.com/
MS Data Converter	AB Sciex	
Proteome Discover 2.1	ThermoFisher Scientific	
SPSS	N/A	https://www.ibm.com/analytics/spss-statistics-software

CONTACT FOR REAGENT AND RESOURCE SHARING

Further information and requests for reagents may be directed to, and will be fulfilled by the Lead Contact, Tao Li (tli@ncba.ac.cn).

EXPERIMENTAL MODELS AND SUBJECT DETAILS

Mice

Trex1^{+/−} C57BL/6 mice were from D. Barnes and T. Lindahl (Cancer Research UK) (Morita et al., 2004; Yang et al., 2007). All animal experiments were performed in accordance with the National Institutes of Health guide for the care and use of laboratory animals and with the approval of the Institutional Animal Care and Use Committee of the National Center of Biomedical Analysis. Stock solutions of aspirin or the control compounds in DMSO was further diluted in PBS containing 5% (vol/vol) Cremophor EL (C5135, Sigma-Aldrich) before intraperitoneal (i.p.) injection. 3-week old *Trex1*^{−/−} mice were given aspirin, salicylic acid, diclofenac sodium, MS-275 or DMSO treatment, respectively. After daily administration for 7 or 10 days, mice were sacrificed and hearts of mice were collected for quantitative polymerase chain reaction (qPCR) analysis of the expression levels of ISGs. Spleens were collected for immunoblot analysis of cGAS acetylation. To evaluate the effect of aspirin on the lethality of *Trex1*^{−/−} mice, 3-week old *Trex1*^{−/−} mice were given daily administration of aspirin, salicylic acid, diclofenac sodium or DMSO for 7 weeks. All the analyses were performed blindly. *Trex1*^{−/−} mice were randomly allocated into experimental groups for further treatment. Cell samples were allocated based on the genotype of interest.

Cells

HEK293T and HeLa cells were cultured in DMEM supplemented with 10% (vol/vol) fetal bovine serum (FBS), 2 mM glutamine, penicillin (100 U/mL) and streptomycin (100 μg/mL). Murine bone marrow cells, THP-1 and L929 cells were cultured in RPMI-1640 medium supplemented with 10% (vol/vol) FBS. 2 mM glutamine, penicillin (100 U/mL) and streptomycin (100 μg/mL).

HEK293T, L929 and PMA (100 ng/mL)-differentiated THP-1 cells were transfected using VigoFect (Vigorous Biotechnology) or Lipofectamine 2000 (Invitrogen) following the manufacture's instructions. For treatment of aspirin or salicylic acid, stock solution was diluted to the final concentrations in Opti-MEM (GIBCO), the pH value of which was adjusted to be under 7 (Charifson and Walters, 2014). The cells were first washed with PBS for three times and then cultured with the aspirin- or salicylic acid-containing Opti-MEM for 1-2 days before further treatment. The cytotoxicity was analyzed by CellTiter 96® AQueous One Solution Cell Proliferation Assay (G3580, Promega) according to the manufacture's instruction.

For cGAMP or c-di-GMP stimulation, cells were incubated for 30 min at 37°C with cGAMP or c-di-GMP in permeabilization buffer (50 mM HEPES pH 7, 100 mM KCl, 3 mM $MgCl_2$, 0.1 mM DTT, 85 mM sucrose, 0.2% BSA, 1 mM ATP and 0.1 mM GTP) with 1 μg/mL digitonin (Sigma, D141). The permeabilization buffer was replaced with RPMI-1640 medium and cells were cultured for indicated time before further analysis.

To make FLAG-cGAS-stable cells, lentiviral stocks were generated in HEK293T. THP-1 cells were transduced with a pCDH-Puro lentivirus carrying FLAG-cGAS expression sequence in the presence of 5 mg/mL polybrene (Sigma-Aldrich). After 24-hour culturing, transduced cells were selected with puromycin (2 μg/mL, Amresco). Endogenous cGAS was deleted in THP1 cells using the lentiCRISPR system. Single-guide RNA (sgRNA) sequences of cGAS were designed by the online tool from Dr. Feng Zhang's lab (http://zlab.bio/guide-design-resources). To rescue the expression of cGAS, *cGAS*^{−/−} THP1 cells were infected with pCDH-CopGFP lentivirus carrying sgRNA-resistant wild-type or the mutant cGAS expression sequences. Rescued cells (GFP[+]) were sorted by flow cytometry (FACS Aria II, BD Biosciences) 3 days after infection. To establish L929-FLAG-m-cGAS stable cells, lentiviral stocks were generated in HEK293T. L929 cells were infected with pCDH-CopGFP lentivirus. Cells that stably expressing FLAG-m-cGAS (GFP+) were sorted by flow cytometry (FACS Aria II, BD Biosciences) 3 days after infection.

THP-1, L929, HeLa and HEK293T cells were obtained from ATCC. All the cell lines have been tested to be mycoplasma-free by PCR.

Viruses

HSV-1 was propagated and titered by plague assay on Vero cells. 6-week old female C57BL/6 mice were given daily administration of aspirin (50 mg/kg) or DMSO for two days before infected with HSV-1 (10^7 *pfu* per mouse) or VSV (10^7 *pfu* per mouse) by i.p. injection. Serum was collected 6 h after viral infection, and was measured for cytokine production by ELISA. All the analyses were performed blindly. Mice were randomly allocated into experimental groups for virus infection.

METHODS DETAILS

Quantitative Polymerase Chain Reaction (qPCR)

Cells were collected and the total RNA was extracted with TRIzol (Thermo Fisher Scientific). The diluted RNA was reverse-transcripted (PrimeScript RT Master Mix, RR036A, TAKARA) and analyzed with qPCR (FastStart Universal SYBR Green Master (Rox), 04913914001, Roche) for the expression of genes on StepOnePlus Real-Time PCR System (Applied Biosystems). The primers were synthesized from Invitrogen and listed in Table S3, *GAPDH* and *Hprt* were used for normalization.

Cell

ELISA

Mice serum was collected and measured for IFN-β concentration using a mouse IFN-β ELISA kit (439408, Biolegend) according to the manufacturer's protocol. PMA-differentiate THP-1 cells were treated with 20 μM diclofenac sodium or DMSO for 24 h and collected for measuring PGE2 concentration using Human PGE2 ELISA kit (EH4233, FineTest).

Isolation of PBMCs from AGS patient

After written informed consent was obtained, we collected the peripheral blood of the patient and his healthy brother with the help of the department of blood transfusion, affiliated hospital of Academy of Military Medical Sciences (AMMS). Human blood samples were obtained following the National Institutes of Health Guide for the use of human samples and with the approval of the Scientific Investigation Board of affiliated hospital of AMMS. Human primary PBMCs were isolated with HISTOPAQUE-1077 (Sigma-Aldrich) according to the manufacturer's protocols. Cells were maintained in RPMI-1640 medium supplemented with 10% (vol/vol) FBS, 2 mM glutamine, penicillin (100 U/mL) and streptomycin (100 μg/mL).

Mass Spectrometry

To identify cGAS acetylation in FLAG-cGAS-expressing THP-1 cells and quantification of HSV-1-induced cGAS acetylation change in these cells, desalting and MS analysis of digested peptides was carried out as previously described (Wang et al., 2014). In brief, de-salted peptides were analyzed using a TripleTOF 5600+ mass spectrometer (AB Sciex) coupled to an ekspert nanoLC 425 (Eksigent). TripleTOF 5600+ raw data were processed using MS Data Converter (AB Sciex) to generate .mgf files. All Mascot searches were performed against a downloaded SwissProt database (released in Jan 2015, 547,357 proteins, 194,874,700 residues) with the taxonomy of *Homo sapiens*. The percentage of acetylation was calculated by peptides counts. The quantification of aspirin-, aspirin-d3- or HT-DNA-induced cGAS acetylation change in FLAG-cGAS-expressing THP-1 cells and aspirin-induced cGAS acetylation in L929-FLAG-m-cGAS cells were performed on the Thermo Scientific Q Exactive HF hybrid quadrupole-Orbitrap mass spectrometer. The MS data were analyzed with Proteome Discover 2.1. The percentage of acetylation was calculated by peptides peak area.

Immunoblotting and Immunoprecipitation

The total cell lysates were prepared in M2 buffer (20 mM Tris-HCl pH 7.5, 0.5% Nonidet P-40, 250 mM NaCl, 3 mM EDTA, 3 mM EGTA, 2 mM dithiothreitol) supplemented with complete protease inhibitor cocktail (Roche, 04693132001). Cell lysates were separated by SDS-PAGE and analyzed by immunoblotting. Proteins were visualized by enhanced chemiluminescence according to the manufacturer's instructions (ThermoFisher Scientific).

To detect cGAS acetylation, cells were lysed in M2 buffer supplemented with complete protease inhibitor cocktail, 1 μM trichostatin A (TSA) and 10 mM nicotinamide (NAM), followed by sonication and centrifugation at 16,000 × g for 10 min at 4°C. The supernatants were immunoprecipitated with cGAS antibody or FLAG antibody for 12 h at 4°C. The immunoprecipitants were washed six times with M2 buffer and boiled in 1 × SDS-loading buffer for immunoblot analysis.

To detect interaction between cGAS and HDACs, cells were lysed in M2 buffer supplemented with complete protease inhibitor cocktail, followed by centrifugation at 16,000 × g for 10 min at 4°C. The supernatants were immunoprecipitated with anti-HDAC3 or anti-FLAG antibody for 12 h at 4°C. The immunoprecipitants were washed six times with M2 buffer and boiled in 1 × SDS-loading buffer for immunoblot analysis.

To detect cGAS acetylation *in vivo*, 3-week old *Trex1*$^{-/-}$ mice were given daily treatment of aspirin (50 mg/kg), salicylic acid (50 mg/kg), diclofenac sodium (1 mg/kg) or DMSO for 1 week by i.p. injection, respectively. Spleens of mice were homogenized with handheld homogenizer (PT 1200 E, Kinematica) and lysed in RIPA buffer (50 mM Tris-HCl pH 7.5, 1% Nonidet P-40, 150 mM NaCl, 5 mM EDTA, 0.5% Deoxycholate Sodium) supplemented with complete protease inhibitor cocktail, 1 μM TSA and 10 mM NAM, followed by sonication and centrifugation at 16,000 × g for 30 min at 4°C. The supernatants were immunoprecipitated with mouse specific cGAS antibody for 12 h and then incubated with Protein G Sepharose (17-0618-01, GE Healthcare) for 3 h at 4°C. The immunoprecipitants were washed six times with RIPA buffer and boiled in 1 × SDS-loading buffer for immunoblot analysis.

Purification of site-specific acetylated cGAS recombinant proteins

The site-specific acetylated cGAS recombinant proteins were generated according to a previous report (Neumann et al., 2008). In brief, *Escherichia coli* strain, BL21 (DE3), was transformed with plasmids pAcKRS-3 and pCDF PylT-1 carrying the ORF for cGAS with an amber codon at the desired site. The cells were first grown overnight in LB medium supplemented with 50 μg/mL kanamycin and 50 μg/mL spectinomycin (LB-KS) at 37°C. 5 mL overnight cultured bacteria were then inoculated into 100 mL LB-KS for further culturing. When the OD$_{600}$ reached 0.4∼0.6, 20 mM nicotinamide (NAM) and 10 mM acetyl-lysine were added and 30 min later, the protein expression was induced at 16-18°C overnight by adding 0.5 mM IPTG. Cells were harvested after induction, and were washed with ice-cold PBS containing 20 mM NAM, the proteins were purified with HisTrap FF (GE Healthcare, 17-5319-01) according to the manufacturer's protocol.

In vitro cGAMP synthesis assay

According to a previously published protocol (Li et al., 2013), unmodified cGAS protein (cGAS^{Non-Ac}) and lysine-acetylated cGAS protein (cGAS^{Lys384Ac}, cGAS^{Lys394Ac}, cGAS^{Lys414Ac} and cGAS^{Lys392Ac}) were incubated with HT-DNA (20 μg/mL) in reaction buffer (20 mM

HEPES, pH 7.5, 5 mM $MgCl_2$, 2 mM ATP, 2 mM GTP) at 37°C for 2 h. The samples were diluted by 5-fold and centrifuged at 16,000 × g for 10 min, and the supernatant was filtered with a 10 kD ultrafiltration filter (Millipore), and analyzed by ion exchange chromatography with a MonoQ column (GE Healthcare).

cGAMP extraction
cGAMP extraction from cells was carried out according to previous report (Wu et al., 2013a). After HT-DNA stimulation, the cells were washed with PBS and lysed with 700 μL of cold extraction solvent (40:40:20 (v/v/v) methanol-acetonitrile-water). The cell lysates were stored at −20°C for 30 min and then centrifuged at 16,000 × g for 5 min. The supernatants were evaporated at room temperature and the pellets were resuspended in 100 μL of ammonium acetate buffer (10 mM ammonium acetate, 0.05% acetate in water). After centrifugation at 16,000 × g for 10 min, the supernatants were quantified by liquid chromatography-MS/multiple reaction monitoring (LC-MS/MRM).

Quantification of cGAMP using LC–MS/MRM
The LC–MS/MS system consisted of an ekspert ultraLC 110-XL system (AB Sciex) and a Qtrap6500 triple quadropole mass spectrometer (AB Sciex). The Qtrap6500 triple quadropole mass spectrometer was operated in positive ionization mode for MRM analysis of cGAMP. The source conditions were set as follows: ionspray voltage was 5.5 kV, ion source temperature was 550°C, curtain gas was 20 (arbitrary units), collision gas was Medium (CAD) and the dwell time for cGAMP was 100 ms. The optimized ion transitions were: cGAMP m/z 675 → 524; m/z 675 → 506; m/z 675 → 136. The parameters, entrance potential (EP), declustering potential (DP), collision energy (CE) and collision exit potential (CXP), were set as 7 V, 90 V, 29 V, and 18 V, respectively.

RNA Interference
For siRNA-mediated knockdown in THP1 cells, siRNAs were electroporated into undifferentiated cells at a final concentration of 100 nM using the Amaxa Transfection Device following the manufacturer's instructions. 24 h after electroporation, cells were differentiated with PMA for 48 h followed by transfection of HT-DNA. For L929 cells, siRNAs were transfected with Lipofectamine RNAiMAX (Invitrogen) at a final concentration of 100 nM. After 24-hour siRNA transfection, cells were treated with aspirin for 48 h. Drug-containing medium was changed every 24 h. Mouse *Dnase2a* (siG151201033118), mouse *Rnaseh2b* (siG170516091413), human *HDAC3* (siB1032283530) and *control* siRNAs were purchased from RiboBio. Mouse *Trex1* (MSS238570, 5′-ACCGACAGA CUCACAUACUGCUGAA-3′) siRNA was from Invitrogen.

IC$_{50}$ Determination
Bone marrow cells from *Trex1*$^{-/-}$ mice were collected and treated with Red Blood Cells Lysis Buffer (155 mM NH_4Cl, 12 mM $KHCO_3$ and 100 μM EDTA). Cells were washed and resuspended in medium containing different concentration of aspirin or salicylic acid. Drug-containing medium was changed every 24 h. 48 h later, cells were collected and the mRNA levels of ISGs were analyzed by qPCR. Data were analyzed by GraphPad Prism and IC$_{50}$ values were calculated with SPSS (Version 21).

DNA Binding Assay
The real-time binding assay was performed by biolayer interferometry using ForteBio Octet red 96. Briefly, Streptavidin (SA) Biosensor from ForteBio were used to capture 20 nM biotin-ISD (biotinylated interferon stimulatory DNA) onto the surface of the SA biosensor. After reaching base line, sensors were subjected to the association step containing 15.625, 31.25, 62.5, 125, 250 or 500 nM His-tagged non-acetylated or acetylated recombinant cGAS proteins for 60 s and then dissociated for 60 s. All reagents were diluted in ForteBio kinetics buffer (50 mM Tris-HCl pH7.5, 150mM NaCl, 0.02% Tween 20, 0.1 mg/mL BSA). Biotin-labeled EGFP-coding sequence (Biotin-EGFP, primer sequences for EGFP cloning are listed in Table S3) was also used as a longer DNA to perform this assay.

Immunofluorescence
To detect the colocalization of HDAC3 and cGAS, human primary macrophages were seeded on coverslips in 24-well plates. After transfection with HT-DNA, the cells were fixed with 4% paraformaldehyde for 15 min, permeabilized with 0.2% Triton X-100 for 10 min, and blocked in 3% BSA for 1 h. Cells were then incubated with primary antibodies (such as rabbit anti-cGAS (Cell Signaling Technology) and mouse anti-HDAC3 (Santa Cruz)) overnight at 4°C,. Alexa Fluor 488- and 546-conjugated secondary antibodies and Hoechst (Life technologies) were incubated for 1 h before the images were acquired using a ZEISS LSM 880 (Zeiss) confocal microscope.

To detect the localization of acetylated cGAS, PMA-differentiated FLAG-cGAS or FLAG-cGAS^{3KQ}-expressing THP1 cells were seeded on coverslips in 24-well plates. After fixed with 4% paraformaldehyde for 15 min, permeabilized with 0.2% Triton X-100 for 10 min, and blocked in 3% BSA for 1 h, cells were then incubated with anti-FLAG antibodies overnight at 4°C. Alexa Fluor 546-conjugated secondary antibody and Hoechst (Life technologies) were incubated for 1 h before the images were acquired using a ZEISS LSM 880 (Zeiss) confocal microscope.

Cell

cGAS dimerization

HEK293T cells were transfected with FLAG-tagged WT cGAS by VigoFect (Vigorous Biotechnology). After 24 h, the cell lysates were prepared in M2 buffer supplemented with complete protease inhibitor cocktail. Cell lysates were then incubated with recombinant His-tagged cGAS proteins, cGAS^{Non-Ac}, cGAS^{Lys384Ac}, cGAS^{Lys394Ac}, or cGAS^{Lys414Ac} for 12 h. Then the cell lysates were incubated with Ni-NTA agarose beads (QIAGEN) for 4 h to pull down His-tagged cGAS proteins. The cGAS-cGAS interaction were analyzed by immunoblotting.

QUANTIFICATION AND STATISTICAL ANALYSIS

No statistical methods were used to estimate sample size. A standard two-tailed unpaired Student's t test was used for statistical analysis of two groups. Statistical analysis of survival curves was performed with a log-rank (Mantel–Cox) test. Statistical analyzed data are expressed as mean ± standard error of the mean (SEM). A p value < 0.05 is considered as statistically significant. We performed the statistical analyses using GraphPad Prism.

DATA AND SOFTWARE AVAILABILITY

All the data are available from the authors upon request.

A

Sites	Peptide sequence	Mascot score	Expect value
K7	MQPWHG**K**(Ac)AMQR	57	0.00014
K50	AG**K**(Ac)FGPAR	61	8.10e-05
K384	LSFSHIE**K**(Ac)EILNNHGK	86	1.40e-08
K392	LSFSHIEKEILNNHG**K**(Ac)SK	129	9.90e-13
K394	LSFSHIEKEILNNHGKS**K**(Ac)	27	0.0037
K414	LM**K**(Ac)YLLEQLK	60	2.10e-05

B

C

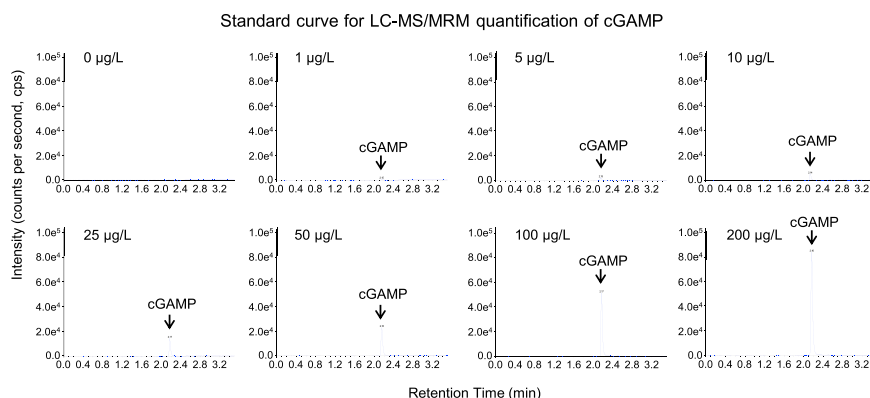Standard curve for LC-MS/MRM quantification of cGAMP
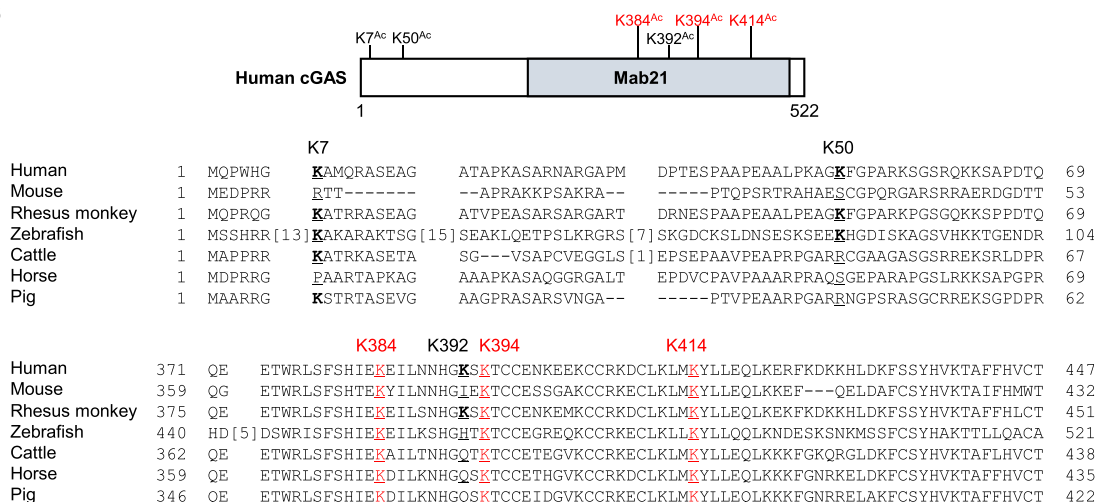
Figure S1. Identification of cGAS Acetylation, Related to Figure 1

(A) List of the identified acetylation sites of cGAS. PMA-differentiated THP-1-FLAG-cGAS cells were harvested and the FLAG-tagged cGAS was immunopre-cipitated and analyzed by Triple-TOF 5600+ mass spectrometer.

(B) cGAS acetylation sites identified with mass spectrometry. The conserved sites (K384, K394 and K414) are highlighted as red.

(C) Commercial 2′,3′-cGAMP with indicated concentrations were used to generated standard curve for LC-MS/MRM quantification.
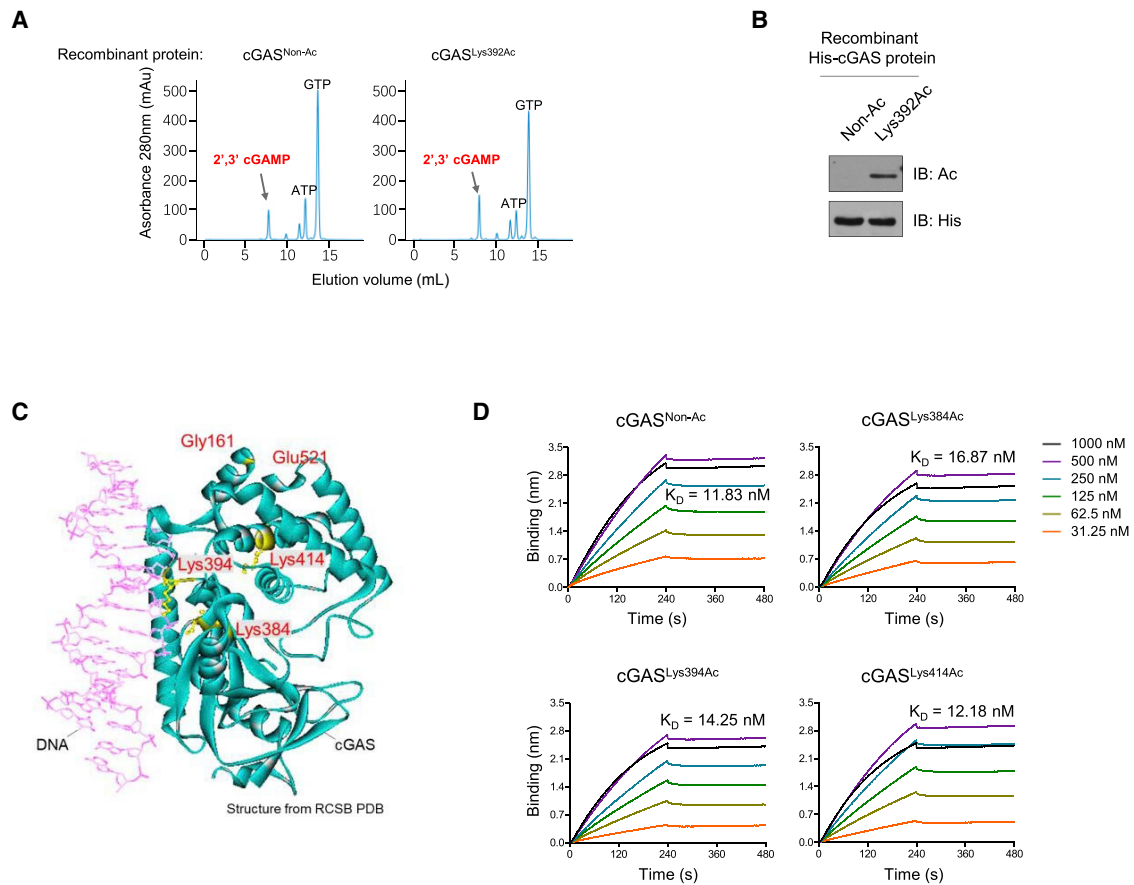
Figure S2. Acetylation Suppresses cGAS Activity, Related to Figure 2

(A) Ion exchange chromatography analysis of cGAMP production in the *in vitro* cGAMP synthesis assay using cGAS[Lys392Ac] and the unmodified cGAS (cGAS[Non-Ac]).

(B) Immunoblot analysis of recombinant cGAS proteins from B with pan-acetyl-lysine antibody. Anti-His blot indicates loading of lanes.

(C) The cGAS structural data were downloaded from RCSB PDB (PDB: 6CT9) and analyzed by Accelrys Discovery Studio client 2.5. K384, K394 and K414 of cGAS are highlighted. The first amino acid (Gly161) and the last amino acid (Glu521) of the truncated cGAS in this structure are also shown.

(D) The real-time association and dissociation of non-acetylated or acetylated recombinant cGAS proteins with biotin-ISD were recorded by ForteBio Octet red 96. Processed kinetic data show binding affinity constants (equilibrium dissociation constant, K_D).

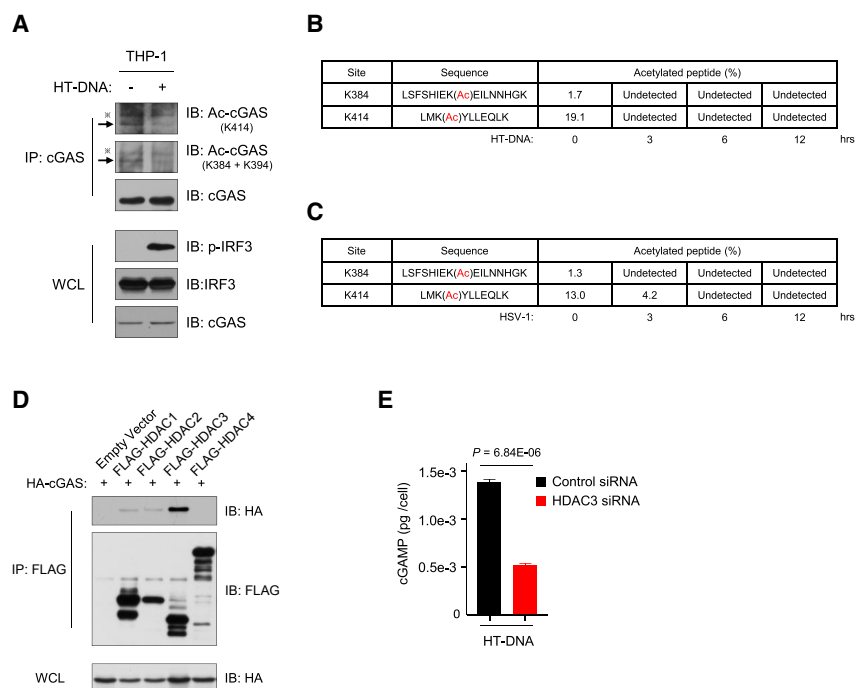Data represent at least two independent experiments (B-D).

A

THP-1

HT-DNA: − +

IP: cGAS
- IB: Ac-cGAS (K414) ※
- IB: Ac-cGAS (K384 + K394) ※
- IB: cGAS

WCL
- IB: p-IRF3
- IB:IRF3
- IB: cGAS

B

Site	Sequence	Acetylated peptide (%)			
K384	LSFSHIEK(Ac)EILNNHGK	1.7	Undetected	Undetected	Undetected
K414	LMK(Ac)YLLEQLK	19.1	Undetected	Undetected	Undetected
	HT-DNA:	0	3	6	12 hrs

C

Site	Sequence	Acetylated peptide (%)			
K384	LSFSHIEK(Ac)EILNNHGK	1.3	Undetected	Undetected	Undetected
K414	LMK(Ac)YLLEQLK	13.0	4.2	Undetected	Undetected
	HSV-1:	0	3	6	12 hrs

D

Empty Vector / FLAG-HDAC1 / FLAG-HDAC2 / FLAG-HDAC3 / FLAG-HDAC4

HA-cGAS: + + + + +

IP: FLAG
- IB: HA
- IB: FLAG

WCL
- IB: HA

E

P = 6.84E-06

cGAMP (pg /cell)

■ Control siRNA
■ HDAC3 siRNA

HT-DNA

Figure S3. DNA Triggers cGAS Deacetylation, Related to Figure 3

(A) PMA-differentiated THP-1 cells were treated with HT-DNA (2 μg/mL) for 3 h. cGAS was immunoprecipitated and the acetylation of cGAS was analyzed with the site-specific cGAS acetylation antibodies as indicated. ※ indicate non-specific bands.

(B and C) FLAG-cGAS-expressing THP-1 cells were differentiated with PMA for 72 h, followed by HT-DNA (B) or HSV-1 (C) treatment for indicated time. FLAG-cGAS was immunoprecipitated for mass spectrometry analysis of acetylation. The percentage of cGAS acetylation at indicated sites was calculated.

(D) HA-tagged cGAS and FLAG-tagged HDACs as indicated were co-expressed in HEK293T cells. The interaction between cGAS and different HDACs was examined by FLAG-immunoprecipitation (IP) and immunoblotting.

(E) THP-1 cells were transfected with either control siRNAs or HDAC3 siRNAs followed by PMA differentiation and a 2-hour HT-DNA (1 μg/mL) treatment. cGAMP production was quantified by LC-MS/MRM, data are mean ± SEM, from triplicates (technical replicates), unpaired t test.

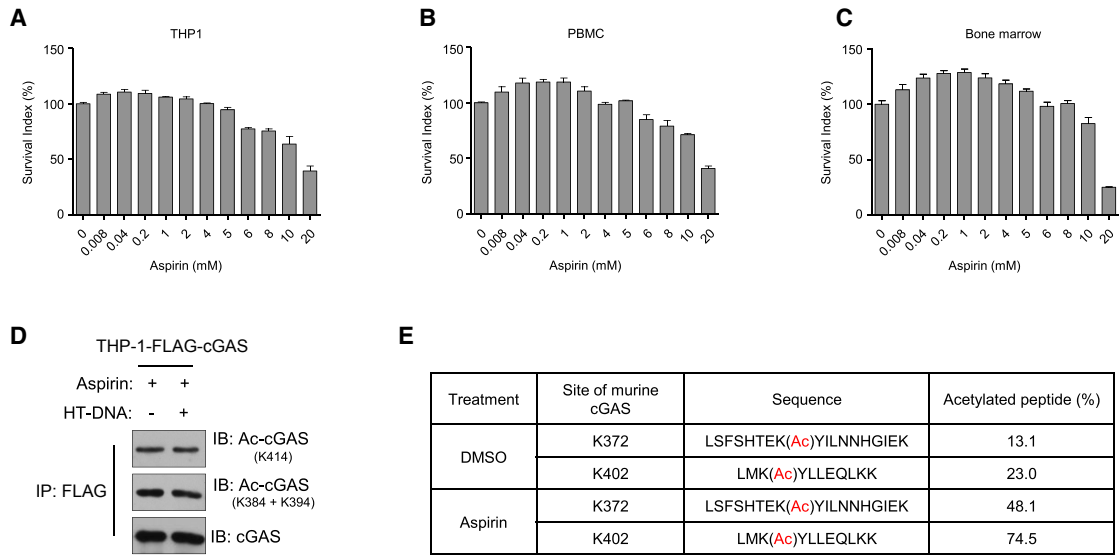WCL, whole cell lysate. Data represent three independent experiments.

A THP1

B PBMC

C Bone marrow

D THP-1-FLAG-cGAS

Aspirin: + +
HT-DNA: - +

IP: FLAG

IB: Ac-cGAS (K414)
IB: Ac-cGAS (K384 + K394)
IB: cGAS

E

Treatment	Site of murine cGAS	Sequence	Acetylated peptide (%)
DMSO	K372	LSFSHTEK(Ac)YILNNHGIEK	13.1
	K402	LMK(Ac)YLLEQLKK	23.0
Aspirin	K372	LSFSHTEK(Ac)YILNNHGIEK	48.1
	K402	LMK(Ac)YLLEQLKK	74.5

Figure S4. Cytotoxicity of Aspirin, Related to Figure 4

(A-C) THP-1 cells (A), human PBMCs (B) and mouse bone marrow cells (C) were plated in 96-well plates and cultured in the presence of aspirin at indicated concentrations for 24 h. The cytotoxicity was analyzed by CellTiter 96® AQueous One Solution Cell Proliferation Assay. Data are mean ± SEM from triplicates (technical replicates).

(D) FLAG-cGAS-expressing THP-1 cells were differentiated with PMA for 72 h, followed by aspirin treatment for 24 h. The cells were then challenged with HT-DNA for 3 h. FLAG-cGAS was immunoprecipitated and cGAS acetylation was analyzed with indicated antibodies.

(E) FLAG-m-cGAS-expressing L929 cells were treated with DMSO or aspirin (4 mM) for 24 h. FLAG-m-cGAS was immunoprecipitated. The K372 and K402 acetylated cGAS peptides were analyzed with Thermo Scientific Q Exactive HF hybrid quadrupole-Orbitrap mass spectrometer.
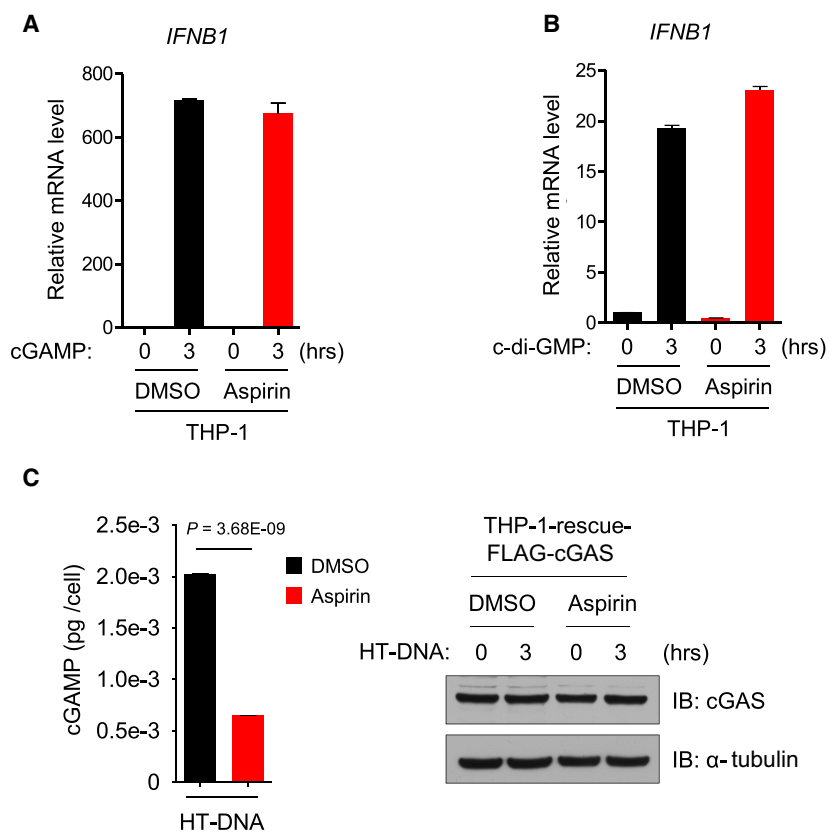
Data represent two independent experiments.

Figure S5. Enforced Acetylation of cGAS by Aspirin Inhibits cGAS-mediated IFN Production, Related to Figure 5
(A and B) PMA-differentiated THP-1 cells were pre-treated with DMSO or aspirin (4 mM) for 24 h followed by the treatment with cGAMP (1 μg/mL) (A) or c-di-GMP (1 μg/mL) (B) for indicated h. qPCR analysis of *IFNB1* mRNA levels in cells. Data are mean ± SEM, from triplicates (technical replicates).
(C) cGAS knock-out THP-1 cells that expressing FLAG-cGAS (THP-1-rescue-FLAG-cGAS) were differentiated with PMA, followed by DMSO or aspirin (4 mM) treatment for 24 h. The cells were treated with HT-DNA (1 μg/mL) for 2 h. cGAMP production was quantified by LC-MS/MRM, data are mean ± SEM, from triplicates (technical replicates), unpaired t test (left). Immunoblot analysis of cGAS in the corresponding protein samples (right). Anti-α-tubulin blot indicates loading of lanes.
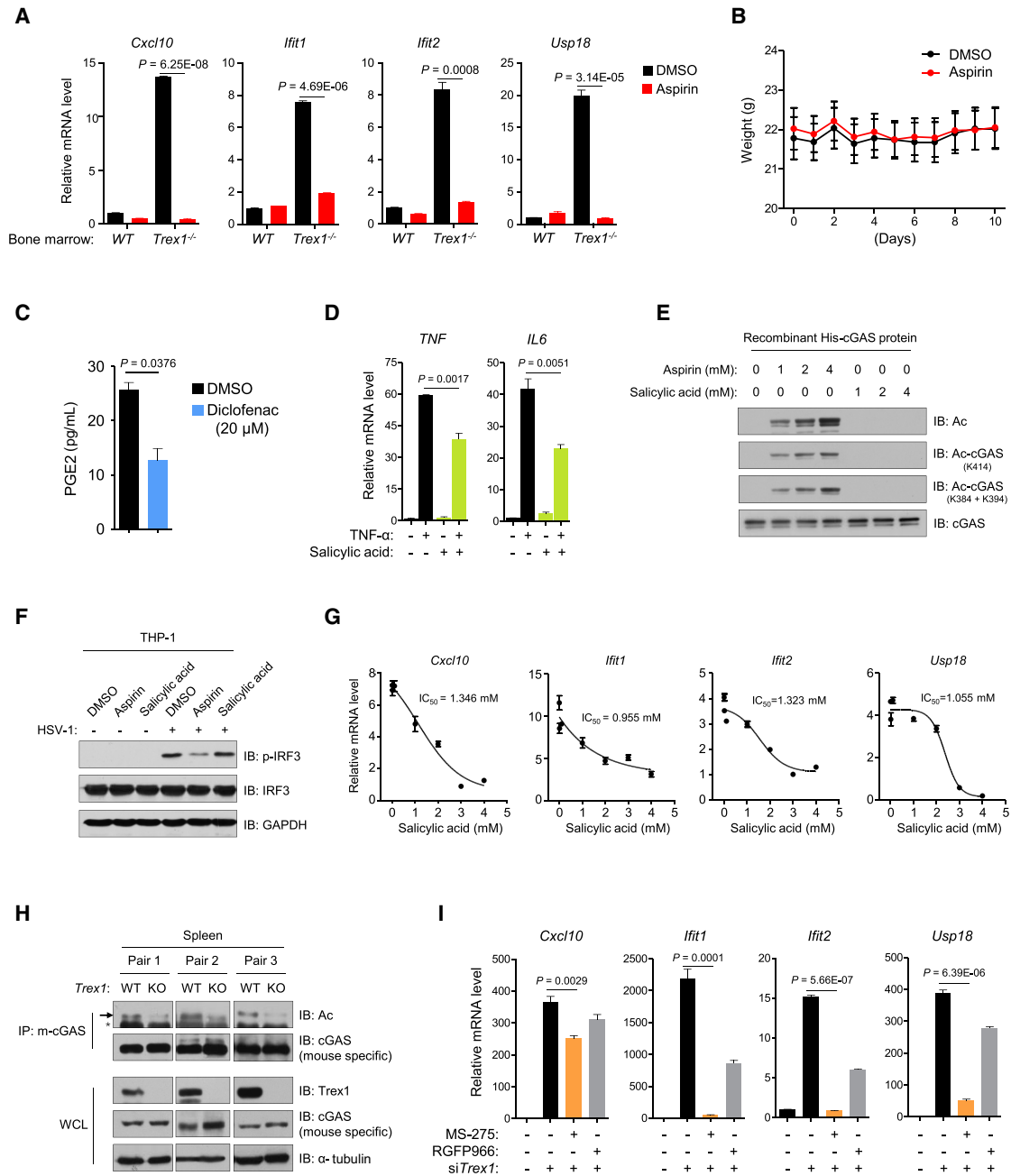Data represent three independent experiments.

Figure S6. Aspirin Suppresses DNA-Mediated Autoimmune Responses, Related to Figure 6

(A) Bone marrow cells from WT and *Trex1*$^{-/-}$ mice were treated with DMSO or aspirin (4 mM) for 2 days. mRNA levels of different ISGs as indicated were detected by qPCR. Data are mean ± SEM, from triplicates (technical replicates), unpaired t test.

(B) Wild-type mice (n = 20) were given daily administration (i.p.) of aspirin (50 mg/kg) or DMSO for 10 days. Body weight of mice were monitored. Data are mean ± SEM.

(C) PMA-differentiated THP-1 cells were treated with DMSO or diclofenac sodium (20 μM) for 24 h. Cells were collected for measuring PGE2 concentration. Data are mean ± SEM, from duplicates (technical replicates), unpaired t test.

(D) HeLa cells were pretreated with salicylic acid (4 mM) for 1 hour, followed by TNF-α (30 ng/mL) treatment for 60 min. mRNA levels of *TNF* and *IL6* were analyzed by qPCR. Data are mean ± SEM, from triplicates (technical replicates), unpaired t test.

(E) Incubation of recombinant cGAS protein with aspirin or salicylic acid. Immunoblot analysis of cGAS acetylation with pan-acetyl-lysine antibody or site-specific cGAS acetylation antibodies.

(F) PMA-differentiated THP-1 cells were infected with HSV-1 (MOI = 10:1) for 6 h after DMSO, aspirin (4 mM) or salicylic acid (4 mM) pretreatment, the phosphorylation of IRF3 was analyzed by immunoblotting. Anti-GAPDH blot indicates loading of lanes.

(G) Bone marrow cells from *Trex1*$^{-/-}$ mice were treated with salicylic acid at indicated concentrations for 2 days. mRNA levels of ISGs as indicated were analyzed by qPCR (relative to that of WT bone marrow cells). The IC$_{50}$ was calculated by SPSS. Data are mean ± SEM from triplicates (technical replicates).

(H) m-cGAS in spleen of wild-type or *Trex1*$^{-/-}$ mice was immunoprecipitated and the acetylation of m-cGAS was analyzed with pan-acetyl-lysine antibody, anti-α-tubulin blots indicate loading of lanes. * indicates non-specific bands. WCL, whole cell lysate.

(I) *Trex1* expression in L929 was knocked down using siRNAs. The cells were then treated with MS-275 (10 μM), RGFP966 (10 μM) or DMSO for 24 h. mRNA levels of different ISGs as indicated were analyzed by qPCR. Data are mean ± SEM, from triplicates (technical replicates), unpaired t test.
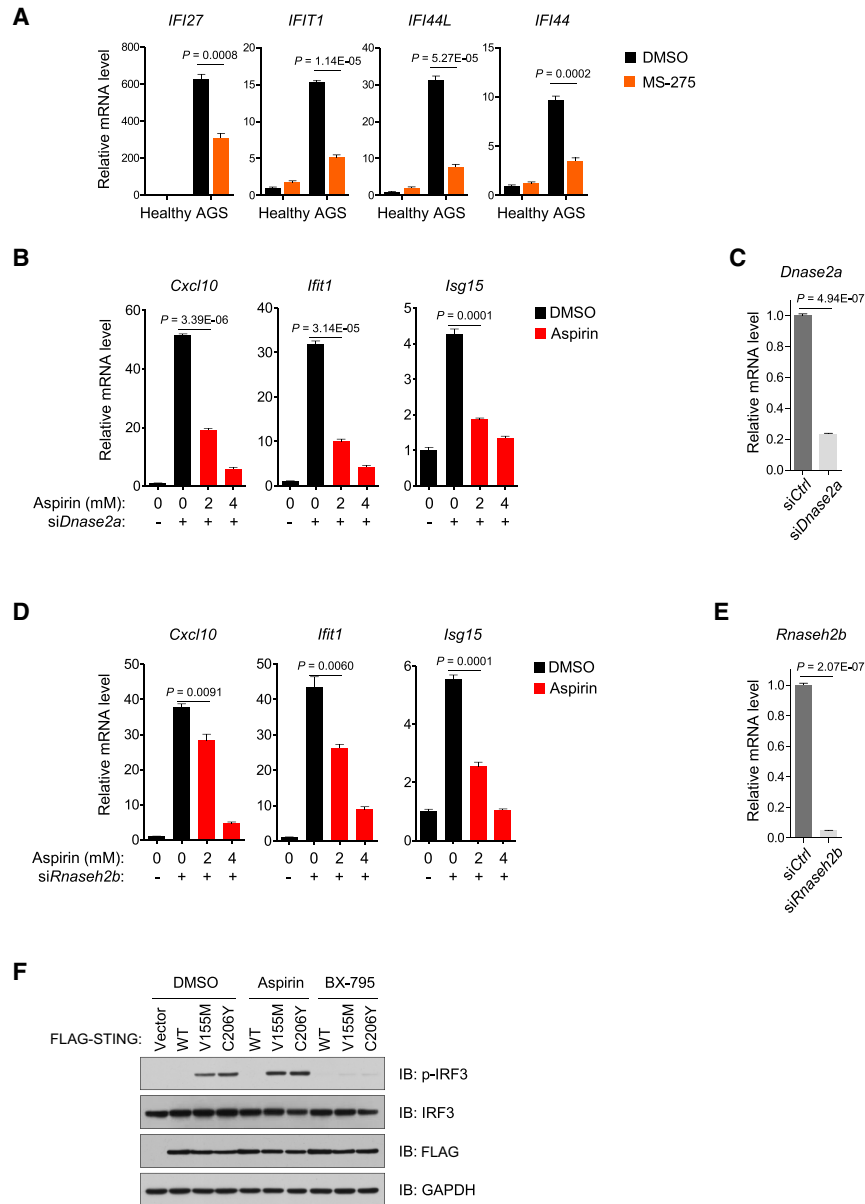
Data represent three independent experiments.

Figure S7. Aspirin Suppresses cGAS-Mediated Type I Interferonopathies, Related to Figure 7

(A) PBMCs from the AGS patient and his healthy brother were treated with DMSO or MS-275 (5 μM) for 24 h. mRNA levels of ISGs were analyzed by qPCR.

(B) Dnase2a-knockdown L929 cells were treated with DMSO or aspirin as indicated for 2 days. mRNA levels of different ISGs as indicated were analyzed by qPCR.

(C) mRNA levels of *Dnase2a* in cells in B was analyzed by qPCR.

(D) Rnaseh2b-knockdown L929 cells were treated with DMSO or aspirin as indicated for 2 days. mRNA levels of different ISGs as indicated were analyzed by qPCR.

(E) mRNA levels of *Rnaseh2b* in cells in D was analyzed by qPCR.

(F) FLAG-tagged wild-type (WT) human STING or its gain-of-function mutants were expressed in HEK293T cells. The cells were then treated with DMSO or aspirin (4 mM) for 24 h, or BX-795 (60 μM) for 6 h. Immunoblot analysis of phosphorylation of IRF3, anti-GAPDH blot indicates loading of lanes.

Data are mean ± SEM, from triplicates (technical replicates), unpaired t test (A-E). Data represent three independent experiments (B-F).